A STUDY ON MICROVESSELS OF HUMAN BREAST CANCER TISSUES EMBEDDED IN EPOXY RESINS

Kukurtchyan, N. S.[a] and Karapetyan, G. R.[a]

Keywords: Microvessels; human breast cancer; light optical microscopy; epoxy resins.

Tumor vasculature is irregularly sized and arranged in a disorganized manner, where they share characteristics of arterioles, capillaries, and venules simultaneously. Studies on microvessels of tissues (from mastopathy to human breast cancer) embedded in Epoxy resins using a light optical microscopy method were performed and human breast cancer microvessel images getting on semithin epoxy slices gave a new opportunity in the studying of this disease.

*Corresponding Authors

E-Mail: sapootraa_a@yahoo.com

[a] H. Buniatian Institute of Biochemistry, of National Academy of Sciences of Republic Armenia, Paruir Sevag str. 5/1, 0014, Yerevan, Republic of Armenia.

INTRODUCTION

The normal microvessels consist of arterioles, capillaries and venules, and form a well-organized, regulated and functional architecture,[1] but tumor vasculature is unorganized and has trifurcations and branches with uneven diameters. The vessel wall structure is also abnormal in tumors.[2] The formation of new blood vessels (angiogenesis) is required for the growth of most tumors. Angiogenesis in breast cancer helps fulfill the metabolic demands of the progressing tumor and plays a critical role in tumor metastasis.

Extensive laboratory data suggest that angiogenesis plays an essential role in breast cancer development, invasion, and metastasis.[3] Angiogenesis precedes the transformation of mammary hyperplasia to malignancy.[1,4] One of the most well-studied angiogenesis factors is called vascular endothelial-derived growth factor (VEGF). VEGF or other angiogenesis factors produced by tumor cells or nearby cells can cause the development of blood vessels that feed the growing tumor.[5,6] Hyperplastic murine breast papillomas and histologically normal lobules adjacent to cancerous breast tissue,[7-9] support angiogenesis in preclinical models, suggesting that angiogenesis precedes transformation of mammary hyperplasia to malignancy. Switch from sprouting angiogenesis to intussusceptive angiogenesis is an escape strategy from radiation-induced damage to the tumor vasculature.[10] Intussusception is another adaptive response of the tumor cells to stress and hypoxia. The transformation of one form of angiogenesis to another one will show the type of transformation of angiogenesis at human breast cancer.

However, it is still not clear how the alterations of large vessels could lead to such changes. This research aims to study microvessels of tissue (from mastopathy to human breast cancer) embedded in Epoxy resins using a light optical microscopy method.

MATERIALS AND METHODS

Reagents and chemicals: powdered paraformaldehyde, osmium tetraoxide, sodium cacodylate trihydrate; 96 % ethyl alcohol, acetone, Epon 812, Epon Hardener MNA, Epon Hardener DDSA, Epon accelerator DNP-30, Azur II and sodium borate were of analytical grade and purchased from Sigma Chemical Co. (USA).

In a current study at surgical procedures of primary operable human breast cancer**,** the biopsies of tissue located close to cancer tissue (3 patients control tissue), core biopsy (1 case of mastopathy), and core biopsy of breast cancer (10 patients) were taken. All procedures involved human subject were approved by the institutional review board/bioethical committee (Erevan State Medical University, RA) conformed to the Legal Aspects of Research Ethics and Science in European Community directive (2001/20/EC

Small pieces of tissue have immediately put in a cold mix of paraformaldehyde in a sodium cacodylate buffer and glutaraldehyde for 12 hours at 4 °C with following post-fixation in 1% OsO_4 solution for 2, then dehydration in ascending series of spirits; saturation in a mixture of acetone and Epon resins of different proportions to make gelatinous capsules were performed. Observation under a light microscope: semithin epoxy sections with up to 1 micrometer thickness were made using ultra cut Reichert (Austria) stained with Azur II (patent 2844 RA)[11] and studied under light microscope supplied with 40 x10 ocular lens.

RESULTS

As have shown the results of our study, using the current method of staining the material (human breast cancer tissue embedded in epoxy resins) by Azur II (patent 2844 RA) gives us very informative images of blood vessels for study.

At mastopathy, the blood vessels have insignificant lumen widening. Some capillaries have sprouted. The tendency of growing angiogenesis occurs.

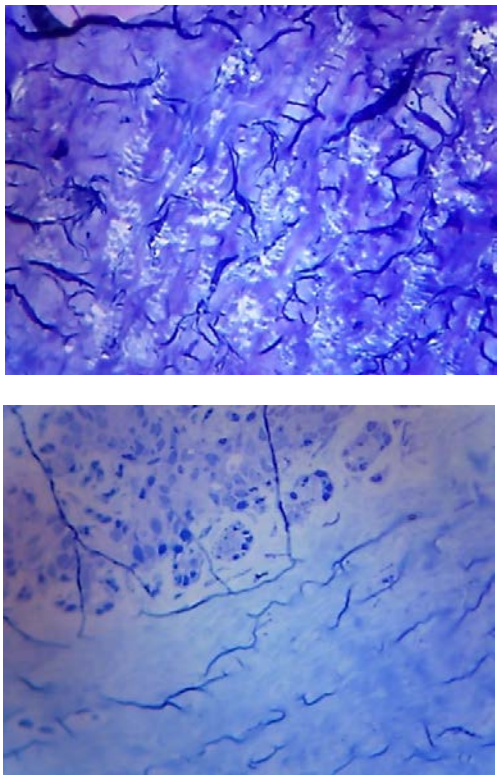

Figure 1. Capillaries at mastopathy

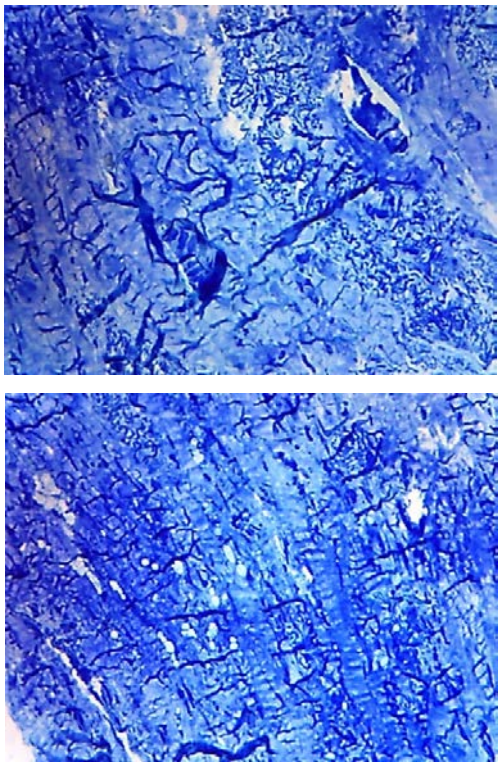

Figure 2. The control tissue of primary operable breast cancer

Blood vessels of breast tissue close to the primary operable tumor are large. Blood capillaries are presented with a high quantity with a different lumen wideness and shape. Many of them have sprouted.

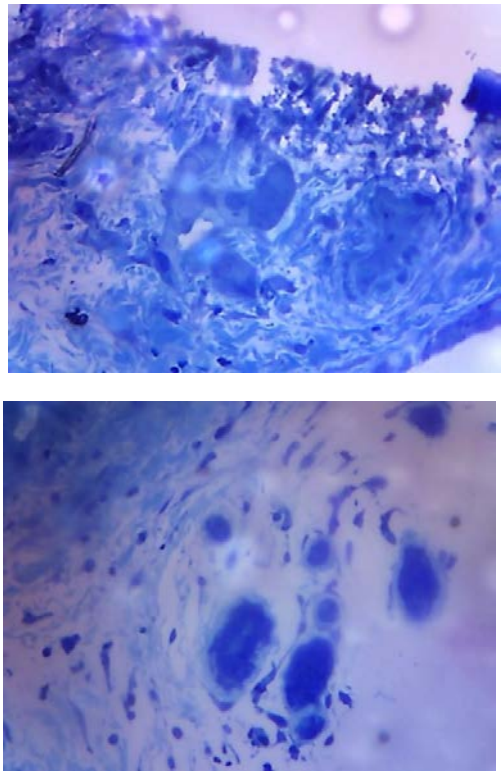

Figure 3. Human breast cancer x400

In studied cases at the II stage of cancer takes place the increasing of the quantity of large vessel profiles by intussusceptions (have one wall and different profiles shape).

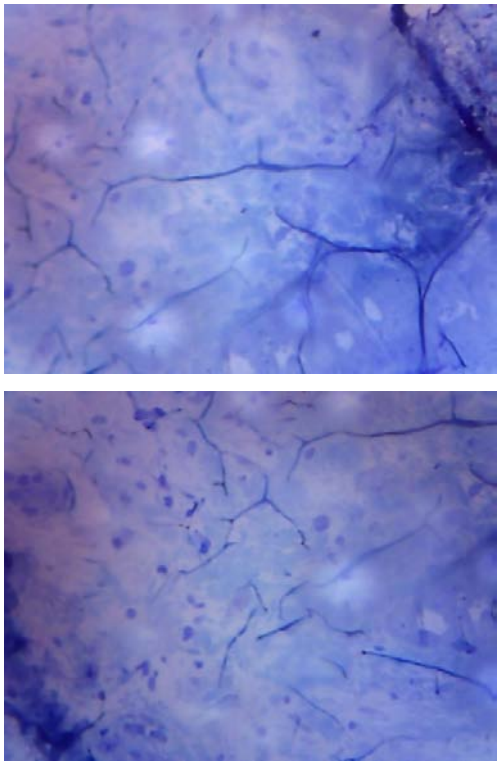

Figure 4. Stage II Human breast cancer tissue

Some of the capillaries with very narrow profile lumen increasing in quantity by intussusceptions. Areas of incompletely divided capillaries are observed.

DISCUSSION

Tumor vasculature is markedly distinct from normal vasculature in that blood vessel that supply tumor tissue are irregularly sized and arranged in a disorganized manner, where they share characteristics of arterioles, capillaries, and venules simultaneously, However, in tumor vasculature, sporadic blood flow is observed, leading to damaged capillary network systems.[12-14] At the same time, the mechanisms leading to it remain unknown.

Angiogenesis in breast cancer helps fulfill the metabolic demands of the progressing tumor and plays a critical role in tumor metastasis. Therefore, various imaging modalities have been used to characterize tumor angiogenesis.[15] Sprouting angiogenesis, the oldest model of microcirculation, is the de novo vessel formation from preexisting blood vessels. Splitting and hijacking, also known, respectively, as intussusception and cooption, are alternative models that account for tumor resistance to antiangiogenic therapy.[5] Despite exposure to antiangiogenic therapy and a subsequent significant decrease in microvascular density, mammary carcinoma had a rapid recovery post-treatment cessation, in virtue of intussusceptive pruning. Intussusceptive vessel growth involves bilateral centripetal protrusion of opposite endothelial cells lining the vessel wall.[16] Once in contact, the opposite vessel walls fuse and tiny apertures in the endothelial lining of the vessel walls form, ultimately leading to the splitting of the two newly formed vessels.[16,17] In contrast to sprouting angiogenesis, splitting angiogenesis is an energy-conserving mechanism as it does not dependent on a high rate of proliferation or basement membrane degradation and invasion, therefore saving energy and permitting the survival of the tumor despite hypoxia and stress.[16,18]

Tumor vasculature may be visualized using parametric imaging of specific morphological and physiological characteristics that collectively describe its properties.[19]

There is still uncertainty about angiogenesis as a prognosticator in breast cancer, with publications of conflicting results.[16] The tumor growth dependency on angiogenesis,[12,20] makes the hypothesis of angiogenesis as a prognosticator attractive.[21] Studies of the assessment of angiogenesis have mainly been based on this hot-spot approach, preferentially using the technique of counting microvessel profiles by all immunohistochemically stained distinct endothelial cells or cell clusters in a microscopic field.[22]

By the way dates of alteration takes place in large vessels are not taken into consideration at this very effective method, which becomes possible by staining of Azur 2 of semithin epoxy slices

In recent studies of tumor samples taken from 66 patients with T1-2 stages of invasive breast cancer of a non-specific type were stained with hematoxylin by Mayer and eosin, as well as by immunohistochemical method using antibodies to CD34 (the focus is on the evaluation of blood capillaries based on methodological facilities).[23] However, practice of tissue staining by Azur II on semithin epoxy slices does not ask using specific markers, sources, or involving additional methods for obtaining vessel images,[11] let us observe the vascular network of microvascular beds.

As have shown the results of this study, the alteration takes place in arterioles by the type of intussusception that can lead to damage to capillary network systems.

Beginning with the canonical sprouting angiogenesis vasculogenesis and intussusception, and finishing with vasculogenic mimicry, the need for different neovascularization mechanisms is further explored.[24]

CONCLUSION

Obtaining human breast cancer microvessels images on semithin epoxy slices gives new opportunities for further study of this disease.

ACKNOWLEDGMENT

Current work was performed by the support H. Buniatian Institute of Biochemistry Natl. Acad. Sci. of RA.

REFERENCES

[1]Jain, R. K., Molecular regulation of vessel maturation. *Nat. Med*., **2003**, *9(6)*, 685-93. DOI: 10.1038/nm0603-685

[2]McDonald, D. M., Choyke, P. L., Imaging of angiogenesis: from microscope to clinic, *Nat. Med*., **2003**, *9(6)*, 713-25. DOI:10.1038/nm0603-713.

[3]Ucuzian, A. A., Gassman, A. A., East, A. T., Greisler, H. P., Molecular Mediators of Angiogenesis. *J. Burn. Care Res*., **2010**, *31(1)*, 58. DOI:10.1097/BCR.0b013e3181c7ed82

[4]Bryan, P., Schneider, K., Miller, D., Angiogenesis of Breast Cancer. *J. Clin. Oncol.*, 2005, 23(8), 1782-1790. DOI: 10.1200/JCO.

[5]Salven, P., Ruotsalainen, T., Mattson, K., Joensuu, H. H., High pretreatment serum level of vascular endothelial growth factor (VEGF) is associated with poor outcome in small-cell lung cancer. *Int. J. Cancer*, **1998**, *79*, 144–146. DOI:10.1002/(sici)1097-0215(19980417)79:2<144::aid-ijc8>3.0.co;2-t

[6]Takahashi, Y., Kitadai, Y., Bucana, C. D., Cleary, K. R., Ellis, L. M., Expression of vascular endothelial growth factor and its receptor, KDR, correlates with vascularity, metastasis, and proliferation of human colon cancer. *Cancer Res*. 1995, 55, 3964–3968.

[7]Brem, S., S., Gullino, P. M., Medina, D., Angiogenesis: A marker for neoplastic transformation of mammary papillary hyperplasia. *Science*, **1995**, *880*, 1977-882,

[8]Carmeliet, P., Jain, R. K., Molecular mechanisms and clinical applications of angiogenesis. *Nature*, **2011**, *473(7347)*, 298-307. DOI: 10.1038/nature10144

[9]Djonoy, V., Andres, A. C., Ziemieski, A., Vascular remodeling during the normal and malignant life cycle of the mammary gland, *Microsc. Res. Tech*., **2001**, *52(2)*, 182-9. DOI: 10.1002/1097-0029(20010115)52:2<182::AID-JEMT1004>3.0.CO;2-M.

[10]Alameddine, R. S., Hamieh, L. and Shamseddine, A., From Sprouting Angiogenesis to Erythrocytes Generation by Cancer Stem Cells: Evolving Concepts in Tumor Microcirculation. *Shamseddine Biomed. Res. Int.*, **2014**, ID 986768. DOI:10.1155/2014/986768

[11]Kukurtchyan, N. S., Karapetyan, G. R., Patent 2844A, Rep. Armenia, **2014.**

[12]Bergers, G., Benjamin, L. E., Tumorigenesis and the angiogenic switch, *Nat. Rev. Cancer*, **2003**, *3*, 401–10. DOI:10.1038/nrc1093

[13]Foikman, J., *Tumor angiogenesis*, Mendelsohn, J., Howley, P. M., Israel, M. A., Liotta, L. A. Eds. *The Molecular Basis of Cancer*, **1995,** 206-232, W. B. Saunders Philadelphia,

[14]Fox, S. B., Tumour angiogenesis and prognosis, *Histopathology*, **1997**, *30, 294-301*. DOI:10.1046/j.1365-2559.1997.d01-606.x

[15]Hanahan, D., Folkman, J., Patterns and emerging mechanisms of the angiogenic switch during tumorigenesis. *Cell*, **1996**, *86*, 353–64. DOI: 10.1016/S0092-8674(00)80108-7

[16]Djonov, V., Baum, O., Burri, P. H., Vascular remodeling by intussusceptive angiogenesis, *Cell Tissue Res.*, **2003**, *314(1)*, 107–117. DOI:10.1007/s00441-003-0784-3

[17]Burri, P. H., Hlushchuk, R., Djonov, V., Intussusceptive angiogenesis: its emergence, its characteristics, and its significance, *Dev. Dyn.*, **2004**, *231*, 474–88. DOI: 10.1002/dvdy.20184

[18]Ribatti, D., Nico, B., Floris, C., Mangieri, D., Piras, F., Ennas, M. G., Vacca, A., Sirigu, P., Microvascular density, vascular endothelial growth factor immunoreactivity in tumor cells, vessel diameter and intussusceptive microvascular growth in primary melanoma. *Oncol. Rep.*, **2005**, *14*, 81–84.

[19]Schatten, H., *Cell and Molecular Biology of Breast Cancer*, https://books.google.com/books?isbn=1627036342. **2013**, Springer Science-Business Media, New York, ISBN 978-1-62703-634-4

[20]Nishida, N., Yano, H., Nishida, T., Kamura, T. and Kojiro, M., Angiogenesis in Cancer, *Vasc. Health Risk Manag.*, **2006**, *2(3)*, 213–219.

[21]Siemann, D. W. The unique characteristics of tumor vasculature and preclinical evidence for its selective disruption by tumor-vascular disrupting agents. *Cancer Treat. Rev.*, **2011**, *37*, 63–74. DOI: 10.1016/j.ctrv.2010.05.001

[22]Hansen, S., Grabau, D. A., Sørensen, F. B., Bak, M., Vach, W. and Rose, C., The Prognostic Value of Angiogenesis by Chalkley Counting in a Confirmatory Study Design on 836 Brest Cancer Patients, *Mol. Oncol., Markers, Clin. Correlates*, **2000**, *6(1)*, 139-146

[23]Nikitenko, N. V., Senchukova, M. A., Tomchuk, O. N., Zaitsev, N. B., Stadnikov, A. A., Mitriako, S. O., Degtearev, A. M., Kirtbaia, D. V., Morphological Characteristic and Clinical Value of Different Types of Tumor Vessels in Breast Cancer, *Bioterap. Zh. Ross.*, **2016**, *15(3)*, 15-22. DOI: 10.17650/1726-9784-2016-15-3-15-22

[24]Zuazo-Gaztelu, I. and Casanovas, O., Unraveling the Role of Angiogenesis in Cancer Ecosystems, *Front. Oncol.*, **2018**, *8*, Article N. 248. DOI: 10.3389/fonc.2018.00248

Received: 02.10.2019.
Accepted: 02.11.2019.

SYNTHESIS AND STUDIES OF SOME *cis*-MoO_2(VI) COMPLEXES WITH NITROGEN DONOR MACROCYCLIC LIGANDS

Ramesh K. Gautam[a], Chandra P. Singh[b], Rajul Saxena[a] and Devendra P. Rao[a]*

Keywords: Dioxomolybdenum(VI), di-2-thienylethanedione, 1,3-diketones, macrocyclic complexes, Schiff base.

A complex of formula $[MoO_2(L)](acac)_2$ is obtained on treating molybdenyl acetylacetonate with di-2-thienylethanedione with 2,3-diaminotoluene This complex was reacted with four 1,3-diketones to yield four new complexes, $[MoO_2(ML)](acac)_2$, The complexes were characterized by elemental analysis, spectral studies and molar conductance. In these compounds, molybdenum exhibited a coordination number of six. Distorted octahedral environment surrounds molybdenum in these complexes. The ligand geometry was completed by two oxo O-atoms and four N-atoms. The synthesized complexes show moderate activity versus S. *aureus* and S. *typhi*.

*Corresponding Authors
E-Mail: devendraprataprao@yahoo.com
[a] Department of Chemistry, D.A-V. (P.G.) College, Kanpur-208001, U.P., India.
[b] Department of Chemistry, D.B.S. (P.G.) College, Kanpur-208006, U.P., India.

INTRODUCTION

A macrocyclic complex is marked as a cyclic complex with at least 9 individuals (counting all hetero atoms) and with at least 3 donor atoms. The field of coordination chemistry of macrocyclic complexes has experienced tremondous improvement during the last quarter of a century.[1-4] A number of reports about synthetic work, physicochemical studies[5] and biochemical applications of metal complexes[6-10] has appeared. Some Schiff bases had been utilized as fungicidal, which has been correlated with their chemical structure.[11-13] One of the examples is the transamination reactions, catalyzed by metals ions template through the formation of intermediate Schiff bases containing vitamin B_6.[14] Schiff base complexes were used as medicines and show e antiviral,[15,16] anti-inflammatory [17] and antitumor activities.[18]

In bioinorganic chemistry, Schiff base complexes are used as artificial models for the metal containing sites in metallo-proteins and enzymes.[19] Various Schiff base ligands show anticancer activity and this activity of their metal complexes is greater in comparison to that of the free ligands.[20,21] Additionally they exhibit catalytic activity in different chemical reactions,[22] surfactant activities[23] and as memory storage devices in electronics.[24-26]

Schiff bases have been used as stable complexes with transition metal in many applications in chemical studies. Intense efforts has been directed to study the transition metal complexes of excessive denticity ligands with a view to obtain the metal complexes of unusual geometry and coordination number.[27] Molybdenum is adaptable in nature because of its diverse oxidation states ranging from –2 to +6 just as coordination numbers which fluctuate from four to eight.[28] The capability of molybdenum to form complexes with nitrogen, oxygen and sulfur containing ligands resulted in development of molybdenum Schiff base edifices that are efficient in homogeneous and heterogeneous reactions.[29-34] The dioxomolybdenum(VI) complexes with high denticity ligands have importance in theoretical and practical chemistry mainly for biological processes. Mo(VI) complex is extracted as molybdate $[MoO_4]^{2-}$ ion in aqueous medium be based on the concentration and pH of the solution. The $[MoO_4]^{2-}$ ion can act as oxygen atom transfer agents.[35] Their O-atom transfer properties play a critical role in functioning of molybdenum oxotransferase.[36,37] It is present in the oxidized states of a number of redox enzymes, in which their active sites consist of a *cis*-dioxomolybdenum moiety.[38-40]

In the second series of transition metals, only molybdenum is crucial for human, animal and vegetation pathogenic microorganisms.[41,42] The Mo(VI) coordination chemistry is interesting because of their catalytic activities and biological properties.[43-46] Physiological functions of oxomolybdoenzymes are set up via molybdenum.[47-49] Di-2-thienylethanedione is a versatile chelating agent. This ligand has two reactive carbonyl groups also which are capable of undergoing Schiff base condensation with several di- and polyamines. Therefore, di-2-thienylethanedione is a useful synthon for the synthesis of macrocyclic ligands.

Some dioxomolybdenum(VI) complexes with high denticity ligands can be synthesized by condensation of di-2-thienylethanedione with a diamine. The synthesized complex has functionality of undergoing cyclization with 1,3-diketones via the metal template impact. It can be prepared, characterized and their provisional structures are supported by way of molar conductivity, elemental analysis, electronic, infrared and nuclear magnetic resonance spectroscopy.

In view of the importance of dioxomolybdenum(VI) cations in oxygen transfer reactions, a new sequence of dioxomolybdenum(VI) macrocyclic complexes have been synthesized. These dioxomolybdenum(VI) macrocyclic complexes with new multidentated ligands derived from

condensation of di-2-thienylethanedione with 3-methylbenzene-1,2-diamine and 1,3-diketones have been synthesized.

EXPERIMENTAL

All chemicals, used in the preparation of Schiff base (ligands) and complexes, were of reagent grade and were used as obtained from business resources. Starting chemicals like [MoO$_2$(acac)$_2$], the diamine, di-2-furanylethanedione and 1,3-diketones (2,4-pentanedione, 1-phenyl-1,3-butanedione, 4,4,4-trifluoro-1-(2-thienyl)-1,3-butanedione, and 1,3-diphenyl-1,3-propanedione were obtained from Aldrich. They were utilized without further purifications.

The elemental examinations of carbon, hydrogen and nitrogen is done for the ligand and MoO$_2$(VI) complexes by using CHN analyser at CRF, NERIST, Nirjuli, Itanagar, Arunachal Pradesh, India,. To estimate nitrogen Kjeldahl's method is used. After decomposition of the complex, molybdenum was assessed gravimetrically by standard technique.[50] Sulfur was estimated as barium sulfate.[51] Uncorrected melting points were determined with the assistance of sulfuric acid bath. The UV-Visible spectra of the complexes have been recorded on Labinda-UV 3000$^+$ UV/VIS spectrophotometer in the 1100 - 220 nm range in ethyl alcohol as solvent at UPTTI Kanpur, U.P., India. IR spectra of the ligand and complexes of MoO$_2$(VI) were recorded at IIT Kanpur on Perkin-Elmer spectrophotometer (10.03.06) in the range of 4000-400 cm^{-1} with KBr pellet. ^{1}HNMR spectra were obtained on JMM ECS-400 (JEOL) spectrometer at 400 MHz with DMSO-d_6 and were expressed in δ (ppm) relative to TMS. TGA/DTA of the parent complex [MoO$_2$(L)](acac)$_2$ were performed on Perkin Elmer (USA) thermal analyzers, under N_2 atmosphere in the temperature range of 50-600 ˚C at the heating rate of 10 ˚C min^{-1}.

Synthesis of MoO$_2$(VI) complexes

A solution of di-2-thienylethanedione (0.5570 g, 2.5 mmol) and 2,3-diaminotoluene (0.61164 g, 5 mmol) in 50 mL ethanol was refluxed. This solution was then added to an ethanolic solution of molybdenyl acetylacetonate (0.81537 g, 2.5 mmol) drop by drop. The reaction mixture was refluxed for 3 h. The solution turned brown. The solid complex formed was filtered and washed with ethanol. The yield was 46 %. This product was placed in ethyl alcohol and treated for 3 h with one of the 1,3-diketones viz. 2,4-pentanedione, 1-phenyl-1,3-butanedione, 4,4,4-trifluoro-1-(2-thienyl)-1,3-butanedione or 1,3-diphenyl-1,3-propanedione, in molar ratio 1:1, to obtain the macrocyclic dirty yellow solid product. TLC was used to ascertain the purity of the products. The 1:1 stoichiometry of Mo and the ligand was confirmed by elemental analyses (Table 1).

Antibacterial activity for the testing of 4-bacterial strains

The antibacterial action of the synthesized complexes of MoO$_2$(VI) was examined by in vitro test. This test was performed against four bacterial strains viz., *Staphylococcus aureus, Salmonella typhi, Enterobacter aerogene* and *Bacillus subtilis.* Cup and agar-well diffusion technique was used for the antibacterial test of synthesized MoO$_2$(VI) complexes.[42-44] Doxycycline was taken as the standard material. For this purpose we made trench having dimensions of 6 mm in diameter inside the agar media with the help of a metallic borer. The concentration of bacterial solution in every channel was 3 × 10^5 colony forming units (CFU) mL^{-1}. The MoO$_2$(VI) complexes were dissolved in D to make an 1 % solution. The concentration of the test complex was 300 µg mL^{-1}. The test samples have been added within the corresponding wells. The rest of the wells were packed with DMSO and antibacterial standard doxycycline (0.05 %). Growth inhibitions were tested after 30 h incubation at 35 ˚C.

RESULTS AND DISCUSSION

The reaction of a mixture of di-2-thienylethanedione, 2,3-diaminotoluene and molybdenyl acetylacetonate in 1:2:1 molar ratio in aqueous ethyl alcohol yielded the macrocyclic complexes of MoO$_2$(VI) with Schiff base. IR frequencies of the ligand and the MoO$_2$(VI) complexes and their assignments are recorded in Table 2.

Lowering of $\nu_{C=N}$ frequencies is the major evidence for the proof of the coordination of nitrogen atoms of azomethine groups to the molybdenum in all macrocyclic complexes.[52-55] The spectral bands placed at 1604-1645 cm^{-1} is related to >C=N absorption, which is usually seen at 1665 cm^{-1} in isolated ligands.[52-54] New absorption band at 508-591 cm^{-1} may be allocated to ν_{Mo-N} vibration,[56] that is absent in free ligands. The linkage of both keto groups of di-2-thienylethanedione via >C=O oxygen with diamines is proved by the presence of >C=N band and the absence of >C=O band around 1710 cm^{-1}.[57,58]

IR spectra of the ligand and its complexes of MoO$_2$(VI) are complex as a result of the nearness of various ring vibrations and C-H vibrations. A wide band located at 3433 cm^{-1} is due to $\nu_{asym\ (N-H)}$ and that at 3065 cm^{-1} is due to $\nu_{sym\ (N-H)}$. Within the complex [MoO$_2$(L)](acac)$_2$ these bands remain unchanged but are absent in complex [MoO$_2$(ML)](acac)$_2$, this implies non-participation of the NH group in the bonding.[59] The dioxomolybdenum(VI) complexes form preferentially a cis-dioxo group because of the preferential usage of the d-orbital for bonding. The dioxomolybdenum(VI) complexes revealed two Mo=O stretching bands at 893-910 cm^{-1} and 964-981 cm^{-1} due to asymmetric and symmetric stretching vibrations of the cis-[MoO$_2$]$^{2+}$ moiety with C_{2V} symmetry.[60] Those two IR spectral bands are allocated to $\nu_{asym(O=Mo=O)}$ and $\nu_{sym(O=Mo=O)}$ vibrations, respectively.[60-66] $\nu_{asym(O=Mo=O)}$ vibrations are lower than ones of $\nu_{sym(O=Mo=O)}$.[67,68]

The presence of acetylacetonate group in the MoO$_2$(VI) complexes is inferred from the bands round 1552 - 1569 cm^{-1} and 1467-1480 cm^{-1}, attibuable to $\nu_{C=O}$and $\nu_{C=C}$ vibrations.[69] Infrared bands of the MoO$_2$(VI) macrocyclic complexes exhibit similar spectral bands. Vibrations of terminal amino groups (the asymmetrical and symmetrical N-H stretching) disappear because of the reaction of the amino groups with carbonyl group of 1,3-diketones in the cyclization process.[69,70]

Table 1. Elemental and physical data of the ligand and MoO_2(VI) complexes.

Complex	Empirical formula	F.W.	Yield, %	M.p., ˚C	Elementary analysis: calculated (found)				
					C%	H%	N%	Mo%	S%
L	$C_{24}H_{22}N_4S_2$	430.59	45	115	66.94 (66.93)	5.14 (5.15)	13.01 (13.00)	--	14.89 (14.87)
$[MoO_2(L)](acac)_2$	$C_{34}H_{36}N_4MoS_2O_6$	756.75	50	125	53.96 (53.98)	4.79 (4.78)	7.40 (7.41)	12.67 (12.64)	8.47 (8.46)
$[MoO_2(ML^1)](acac)_2$	$C_{39}H_{40}N_4MoS_2O_6$	820.84	52	110	57.06 (57.05)	4.91 (4.91)	6.82 (6.81)	11.68 (11.69)	7.81 (7.80)
$[MoO_2(ML^2)](acac)_2$	$C_{44}H_{42}N_4MoS_2O_6$	882.91	53	120	59.85 (59.86)	4.79 (4.78)	6.34 (6.34)	10.86 (10.85)	7.26 (7.24)
$[MoO_2(ML^3)](acac)_2$	$C_{42}H_{37}N_4MoO_6S_3F_3$	942.91	58	118	53.50 (53.48)	3.95 (3.96)	5.94 (5.95)	10.17 (10.16)	10.20 (10.22)
$[MoO_2(ML^4)](acac)_2$	$C_{49}H_{44}N_4MoS_2O_6$	944.98	55	122	62.28 (62.29)	4.69 (4.67)	5.92 (5.90)	10.15 (10.14)	6.78 (6.75)

L= ligand derived via condensation of di-2-thienylethanedione with 2,3-diaminotoluene (1:2)
ML^1 = macrocyclic ligand derived via condensation of ligand (L) with 1,3-diketone: 2,4-pentanedione;
ML^2 = macrocyclic ligand derived via condensation of ligand (L) with 1,3-diketone: 1-phenyl-1,3-butanedione
ML^3 = macrocyclic ligand derived via condensation of ligand (L) with 1,3-diketone: 4,4,4-trifluoro-1-(2-thienyl)-1,3-butanedione
ML^4 = macrocyclic ligand obtained by the reaction of ligand (L) with dibenzoylmethane

Table 2. IR spectral bands (ν cm^{-1}) of the ligand and dioxomolybdenum complexes.

Complex	$\nu_{C=N}$	ν_{Mo-N}	$\nu_{C=O}$ of acac	$\nu_{C=C}$ of acac	ν_{asym} (O=Mo=O)	ν_{sym} (O=Mo=O)	ν_{asym} (N-H)	$\nu_{sym(N-H)}$
L	1665s	---	---	---	---	---	3323br	3130br
$[MoO_2(L)](acac)_2$	1604s	508m	1569s	1467m	893s	981s	3433br	3065br
$[MoO_2(ML^1)](acac)_2$	1645m	580m	1555m	1470m	902s	975s		
$[MoO_2(ML^2)](acac)_2$	1640s	591s	1564s	1480s	905m	964s		
$[MoO_2(ML^3)](acac)_2$	1644m	585s	1552m	1475m	910s	965m		
$[MoO_2(ML^4)](acac)_2$	1640s	524m	1560s	1472m	902m	968s		

^{1}H NMR spectrum of the free ligand exhibits signal of NH_2 protons at 5.80 which is present in $[MoO_2(L)](acac)_2$ at 5.10 but missing in the four macrocyclic complexes $[MoO_2(ML)](acac)_2$ which indicates a cyclization by 1,3-diketones. The ten protons present as multiplets inside the range of 7.06-7.84 for the ligand and molybdenum complexes.

The protons of aromatic ring appeared by peaks at about 7.26. ^{1}H NMR signal about 3.29-3.82 are due to the CH_2N fragment. These chemical shifts might be a direct result of arrangement of two types of azomethine that is ingaged in the formation of the macrocyclic complex. The sharp singlet signal at 2.47 might be because of the water present in DMSO-d_6 sample used. The ^{1}H NMR data of the ligand and complexes are summarized in Table 3.

The UV-Vis spectra of the tetradentate tetraaza ligand and the dixomolybdenum(VI) complexes had been recorded in ethanol and these spectral bands are consistent with suggested strength energy level scheme.[71,72] The spectra of the dixomolybdenum(VI) complexes with tetradentate ligand are comparable to each other thereby suggesting a common structure for all. In view of the fact that Mo(VI) ion has no d-electron, the absorption bands of pure d-d origins are not expected to appear. The bands for all complexes may perhaps to be attributed to charge transfer transition from nitrogen orbital to a molybdenum metal d-orbital [N(π)→*d*(Mo)]. The UV-VIS spectra are similar to those of other complexes of dioxomolybdenum(VI) having nitrogen donor atoms. The UV-VIS spectra of these complexes are distinguished by strong absorption bands within the UV region at ≈ 292 nm and at ≈ 311 nm, which appear to be due to intraligand transition and $n\rightarrow\pi^*/\pi\rightarrow\pi^*$ transitions. A fairly intense band appearing in the vicinity of ≈380-395 nm is attributed to N(π)→*d*(Mo).

Table 3. ^{1}HNMR spectral data of the ligand and dioxomolybdenum complexes (in δ ppm).

Complex	HC-Ar	N-H	C-H_3	C-H
L	7.12 10H	5.80 4H	--	--
$[MoO_2(L)](acac)_2$	7.74 10H	5.10 4H	2.46 12H	5.71 2H
$[MoO_2(ML^1)](acac)_2$	7.42 10H	--	2.69 12H	5.58 2H
$[MoO_2(ML^2)](acac)_2$	7.06 10H	--	2.45 12H	5.70 2H
$[MoO_2(ML^3)](acac)_2$	7.84 10H	--	2.70 12H	5.52 2H
$[MoO_2(ML^4)](acac)_2$	7.15 10H	--	2.49 12H	5.58 2H

Table 4. Antibacterial activities of the MoO$_2$(VI) complexes.

Complex	*Staphylococcus aureus*	*Enterobacter aerogenes*	*Salmonella typhi*	*Bacillus subtilis*	Doxycycline
[MoO$_2$(L)](acac)$_2$	17	17	19	20	26
[MoO$_2$(ML^1)](acac)$_2$	14	20	17	22	23
[MoO$_2$(ML^2)](acac)$_2$	14	17	16	20	24
[MoO$_2$(ML^3)](acac)$_2$	15	19	19	--	25
[MoO$_2$(ML^4)](acac)$_2$	17	19	--	22	25

The band due to the transition $^2B_2 \rightarrow {}^2A_1$ ($d_{xy} \rightarrow d_{x2\text{-}y2}$) is perhaps covered by the above bands and ought be attributed to L→M charge - transfer transition among the lowest unoccupied molybdenum d-orbital and highest occupied ligand molecular orbital.[73,74] Ballhausen-Gray energy level diagram is applicable to the energy level scheme for these complexes. The electronic spectra represent a distorted octahedral configuration for all the complexes.[75]

Molar conductance and magnetic and measurements

These complexes are diamagnetic, as obvious for d^0 configuration. Since no electron is present in d-orbital, no d-d transitions are observed for these complexes. The molar conductivity (Λ_M) values for all MoO$_2$(VI) complexes in DMF at ca. 10^{-3} molar solution indicate to be 1:1 electrolytes. The conductance (Λ_M) estimations of prepared MoO$_2$(VI) complexes ranges between the 100 - 115 Ω^{-1} cm^2 mol^{-1}. The molar conductance supports the tentative structures of dioxomolybdenum(VI) complexes of the type (I) and macrocyclic complexes of the type (II) as shown in the schemes.

Thermogravimetric analyses

The thermogravimetric investigation of [MoO$_2$(L)](acac)$_2$ complex has been studied in the temperature range of 50-600 °C at the rate of 10 °C min^{-1}. No apparent decomposition ocurred beneath 170 °C. The [MoO$_2$(L)](acac)$_2$ complex undergoes decay in one step. After that it ignites and decomposes giving a sharp weight loss.

Antibacterial activity

The MoO$_2$(VI) complexes had been tested for antibacterial test towards *Staphylococcus aureus*, *Bacillus subtilis*, *Enterobacter aerogenes* and *Salmonella typhi* (Table 5). The higher in the antibacterial activity of the dioxomolybdenum(VI) complexes can be explained on the basis of chelation hypothesis.[47,48] The reference material was doxycycline. Nearly all the complexes showed low to moderate activity towards *S. aureus* and *S. typhi.*

CONCLUSIONS

In absence of crystal structure study, which is due to of the amorphous nature of the synthesized molecules, we cannot suggest exact structures of these compounds. However, in view of the elemental and spectral studies, we suggest that all the synthesized complexes may be represented as [MoO$_2$(L)](acac)$_2$ and [MoO$_2$(ML^1)](acac)$_2$. The study of antibacterial activity indicated that the complexes are biologically active.

The present study established new synthetic paths to get novel dioxomolybdenum(VI) complexes with Schiff base. The applied spectroscopic methods confirmed the condensation of di-2-thienylethanedione, which is a flexible chelating agent having two responsive carbonyl groups, with diamines and their cyclizations with 1,3-diketones leading to the formation of macrocyclic products of assured geometry around MoO$_2$(VI) centre. The arrangement around Mo is distorted octahedral geometry. The kinetic template impact of dioxomolybdenum(VI) cation assumes a considerable function in the condensation of Schiff base using diamines and di-2-thienylethanedione in ethanol. Bonding of the metal ion with the azomethine N-atoms proved that Schiff bases act as tetradentate ligands. The analytical data confirmed the existence of one metal ion per ligand molecule. The distorted octahedral shape have been suggested for all the prepared cis- MoO$_2$(VI) complexes.

ACKNOWLEDGMENTS

The authors want to thank the Secretary, Board of Management, D.A.V. P.G. College, Kanpur, U.P., India for providing laboratory facilities to work. Analytical facilities extended by IIT Kanpur and UPTTI Kanpur India are gratefully acknowledged.

REFERENCES

[1]Healy, M. D. S., Rest, A. J., Template Reactions, *Adv. Inorg. Chem. Radiochem.*, **1978**, *21*, 1-40. https://doi.org/10.1016/S0065-2792(08)60277-0

[2]Melson, G. A., *Coordination Chemistry of Macrocyclic Compounds*, New York, **1979**.

[3]Lindoy, L. F., Busch, D. H., *Preparative Inorganic Reactions*, vol. *6*, 1. Ed.: Jolly, John Wiley & Sons, **1971**, ISBN 10: 0471446882; ISBN 13:9780471446880

[4]Lindoy, L. F., Busch, D. H., Metal ion controlled syntheses of novel five-coordinate zinc and cadmium complexes containing a helical coordination geometry and their template reaction to form complexes of a pentadentate macrocyclic ligand, *Inorg. Chem.*, **1974**, *13(10)*, 2494-2498. https://doi.org/10.1021/ic50140a037

[5]Luo, X. F., Hu, X., Zhao, X. Y., Goh, S. H., Li. X. D., Miscibility and interactions in blends and complexes of poly(4-methyl-5-vinylthiazole) with proton-donating polymers, *Polymer*, **2003,** *44(18*), 5285. https://doi.org/10.1016/S0032-3861(03)00578-0

[6]Murthy, A. S. N., Reddy, A. R., Electronic absorption spectroscopic studies of enolimine-ketoamine equilibria in Schiff bases, *J. Chem. Sci*., **1981,** *90*(*6*), 519.

[7]Razakantoanina, V., Phung, N. K. P., Jaureguiberry, G., Antimalarial activity of new gossypol derivatives, *Parasitol. Res.*, **2000,** *86*(*8*), 665. https://doi.org/10.1007/PL00008549

[8]Royer, R. E., Deck, L. M., Vander Jagt, T. J., Synthesis and anti-HIV activity of 1,1'-dideoxygossypol and related compounds, *J. Med. Chem*., **1995,** *38*(*13*), 2427. https://doi.org/10.1021/jm00013a018

[9]Flack, M. R., Pyle, R. G., Mullen, N. M., Oral gossypol in the treatment of metastatic adrenal cancer, J. *Clin. Endocrinol. Metab*., **1993,** *76*, 1019. https://doi.org/10.1210/jcem.76.4.8473376

[10]Baumgrass, R., Weiwad, M., Erdmann, F., Reversible inhibition of calcineurin by the polyphenolic aldehyde, gossypol, *J. Biol. Chem.*, **2001,** *276*(*51*), 47914. https://doi.org/10.1074/jbc.M103273200

[11]Al-Shihri, A. S. M., Abdel Fattah, H. M., Thermogravimetric and Spectroscopic characterization of trivalent lanthanide chelates with some Schiff base, *J. Therm. Anal. Calorim*, **2003,** *71*(*2*), 643. https://doi.org/10.1023/A:1022880615841

[12]Raman N., Sakthivel A., Rajasekaran, K., Synthesis and spectral characterization of antifungal sensitive Schiff base transition metal complexes, *Mycobiology*, **2007**, *35(3)*, 150. https://doi.org/10.4489/MYCO.2007.35.3.150

[13]Creaven, B. C., Czeglédi, E., Devereux, M., Enyedi, É. A., Foltyn-Arfa Kia, A., Karcz, D., McClean, S., Nagy, N. V., Noble, A., Rockenbauer, A., Szabó-Plánka, T., Walsh, M., Biological activity and coordination modes of copper(II) complexes of Schiff base-derived coumarin ligands, *Dalton Trans.*, **2010,** *39(45)*, 10854. https://doi.org/10.1039/c0dt00068j

[14]Doctor, V. M., Oro, J., Mechanism of non-enzymtic transition reaction between histidine and alphaoxoyglutaric acid, *J. Biochem.*, **1969,** *112*(5), 691. https://doi.org/10.1042/bj1120691

[15]Jarrahpour, A., Khalili, D., De Clercq, E., Salmi, C., Brunel, J. M., Synthesis, antibacterial, antifungal and antiviral activity evaluation of some new bis-Schiff bases of isatin and their derivatives, *Molecules*, **2007**, *12(8)*, 1720. https://doi.org/10.3390/12081720

[16]Bharti, S. K., Patel, S. K., Nath, G., Tilak, R., Singh, S. K., Synthesis, characterization, DNA cleavage and in vitro antimicrobial activities of copper(II) complexes of Schiff bases containing a 2,4-disubstituted thiazole, *Transit. Met. Chem.*, **2010,** *35(8)*, 917. https://doi.org/10.1007/s11243-010-9412-8

[17]Manjunatha, M., Naik, V. H., Kulkarni, A. D., Patil, S. A., DNA cleavage, antimicrobial, antiinflammatory anthelmintic activities, and spectroscopic studies of Co(II), Ni(II), and Cu(II) complexes of biologically potential coumarin Schiff bases, *J. Coord. Chem.*, **2011**, *64(24)*, 4264. https://doi.org/10.1080/00958972.2011.621082

[18]Amer, S., El-Wakiel, N., El-Ghamry, H., Synthesis, spectral, antitumor and antimicrobial studies on Cu(II) complexes of purine and triazole Schiff base derivatives, *J. Mol. Struc.*, **2013**, *1049*, 326. https://doi.org/10.1016/j.molstruc.2013.06.059

[19]Ohashi, M., Koshiyama, T., Veno, T., Yanase, M., Fujii, H., Watanabe, Y., Preparation of artificial metalloenzymes by insertion of Chromium(III) Schiff base complexes in to apomyoglobin mutants, *Angew. Chem. Int. Ed*., **2003**, *42*(*9*), 1005. https://doi.org/10.1002/anie.200390256

[20]Dongfang, X. X .V., Shuzhi, M. A., Guangyinng, D. V., Qizhuang, H. E., Dazhi, S., Synthesis,Characterization and anticancer properties of rare earth complexes with Schiff base and O-phenanthroline, *J. Rare Earth*., **2008,** *26(5)*, 643. https://doi.org/10.1016/S1002-0721(08)60153-2

[21]Etain, S. E., Abd El-Aziz, D. M., Abd El-Zaher, E. H., Ali, E. A., Synthesis spectral, antimicrobial and antitumor assessment of Schiff base derived from 2-aminobenzothiazol and its transition metal complexes, *Spectrochim. Acta. Mol. Biomol. Spectr. A.*, **2011**, *79(5)*, 1331. https://doi.org/10.1016/j.saa.2011.04.064

[22]Cozzi, P. G., Metal-Salen Schiff base complexes in catalysis: practicalaspects, *Chem. Soc. Rev*.., **2004,** *33(7)*, 410. https://doi.org/10.1039/B307853C

[23]Singh, R. K., Kukrety, A., Saxena, R. C., Thakre, G. D., Atray, N., Ray, S. S., Novel Triazine Schiff Base-Based Cationic Gemini Surfactants: Synthesis and their evaluation as antiwear, antifriction, and anticorrosive additives in polyol, *Ind. Eng. Chem. Res.*, **2016,** *55(9)*, 2520. https://doi.org/10.1021/acs.iecr.5b04242

[24]Sathya, N., Raja, G., Padma Priya, N., Jayabalakrishnan, C., Ruthenium(II) complexes incorporating tridentate Schiff base ligands: Synthesis, spectroscopic, redox, catalytic and biological properties, *Appl. Organomet. Chem.*, **2010,** *24(5)*, 366. https://doi.org/10.1002/aoc.1621

[25]Arun, V., Sridevi, N., Robinson, P. P., Manju, S., Yusuff, K. K. M., Ni(II) and Ru(II) Schiff base complexes as catalysts for the reduction of benzene, *J. Mol. Catal. A Chem.*, **2009,** *304(1-2)*, 191. https://doi.org/10.1016/j.molcata.2009.02.011

[26]Segura, J. L., Mancheño, M. J., Zamora, F., Covalent organic frameworks based on Schiff-base chemistry: synthesis, properties and potential applications, *Chem. Soc. Rev*.., **2016,** *45(20)*,5635. https://doi.org/10.1039/C5CS00878F

[27]Yadav, H. D. S., Sengupta, S. K., Tripathi, S. C., Syntheses and spectroscopic studies on dioxouranium(VI), oxovanadium(IV) and oxozirconium(IV) complexes with tetradentate macrocyclic ligands, *Inorg. Chim. Acta*, **1987**, *128*, 1. https://doi.org/10.1016/S0020-1693(00)84685-X

[28]Crans, D. C., Fifteen years of dancing with vanadium, *Pure Appl. Chem*., **2005**, *77***,** 1407.

https://doi.org/10.1351/pac200577091497

[29]Bagherzadeh, M., Latifi, R., Tahsini, L., Amani, V., Ellern, A., Woo, L. K., Synthesis, characterization and crystal structure of a dioxomolybdenum (VI) complex with a N,O type bidentate Schiff base ligand as a catalyst for homogeneous oxidation of olefins, *Polyhedron*, **2009,** *28(12)*, 2517. https://doi.org/10.1016/j.poly.2009.05.036

[30]Moradi-Shoeili, Z., Zare, M., Bagherzadeh, M., Kubicki, M., Boghaei, D. M., Synthesis, structural characterization, and catalytic reactivity of a new molybdenum(VI) complex containing 1,3,4-thiadiazole derivative as a tridentate NNO donor ligand, *J. Coord. Chem*., **2015,** *68(3)*, 548. https://doi.org/10.1080/00958972.2014.993321

[31]Bagherzadeh, M., Amini, M., Parastar, H., Synthesis, X-ray structure and oxidation catalysis of a oxido–peroxido molybdenum(VI) complex with a tridentate Schiff base ligand, *Inorg. Chem. Commun*., **2012,** *20*, 86. https://doi.org/10.1016/j.inoche.2012.02.023

[32]Aziz, A. A. A., Synthesis, spectroscopic characterization, thermal studies, catalytic epoxidation and biological activity of chromium and molybdenum hexacarbonyl bound to a novel N_2O_2 Schiff base, *J. Mol. Struct*., **2010**, *979(1-3)*, 77. https://doi.org/10.1016/j.molstruc.2010.06.004

[33]Chakravarthy, R. D., Suresh, K., Ramkumar, V., Chand, D. K., New chiral molybdenum complex catalyzed sulfide oxidation with hydrogen peroxide, *Inorg. Chim. Acta*., **2011,** *376(1)*, 57.https://doi.org/10.1016/j.ica.2011.05.033

[34]Rayati, S., Rafiee, N., Wojtczak, A., cis-Dioxo-molybdenum (VI) Schiff base complexes: Synthesis, crystal structure and catalytic performance for homogeneous oxidation of olefins, *Inorg. Chim. Acta*., **2015,** *386*, 27. https://doi.org/10.1016/j.ica.2012.02.005

[35]Pushie, M. J., George, G. N., Spectroscopic studies of molybdenum and tungsten enzymes, *Coord. Chem. Rev*., **2011**, *255(9-10)*, 1055. https://doi.org/10.1016/j.ccr.2011.01.056

[36]Rao, C. P., Sreedhara, A., Rao, P. V., Verghese, M. B., Rissanen, K., Kolehmainen, E., Lokanath, N. K., Sridhar, M. A., Prasad, J. S., Syntheses, structure, reactivity and species recognition studies of oxo-vanadium(V) and -molybdenum(VI) complexes, *J. Chem. Soc*., **1998**, *14*, 2383. https://doi.org/10.1039/a801226a

[37]Hahn, R., Herrmann, W. A., Artens, G. R. J., Kleine, M., Biologically relevant metal coordination compounds: $Mo^{VI}O_2$ and nickel(II) complexes with tridentate aromatic schiff bases, *Polyhedron*, **1995,** *14(20-21)*, 2953. https://doi.org/10.1016/0277-5387(95)00133-D

[38]Mendel, R. R., Bittner, F., Cell biology of molybdenum, *Biochim. Biophys. Acta Mol. Cell Res*., **2006**, *1763(7)*, 621. https://doi.org/10.1016/j.bbamcr.2006.03.013

[39]Sigel, A., Sigel, H., *Metal Ions in Biological Systems, Molybdenum and Tungsten: Their Roles in Biological Processes*, Marcel Dekker, New York, **2002,** 39. https://doi.org/10.1201/9780203909331

[40]Maurya, R. C., Shukla, B., Pandey, A., Synthesis, magnetic, and spectral studies of cis-dioxomolybdenum(VI) complexes derived from N,O- and N_2O_2-type Schiff bases, *Indian J. Chem.*, **2002,** *41A*, 554.

[41]Rousso, L., Friedman, N., Sheves, M.,Ottolenghi, M., pK_a of the protonated Schiff base and aspartic 85 in the bacteriorhodopsin binding site is controlled by a specific geometry between the two residues, *Biochemistry*, **1995**, *34(37)*, 12059. https://doi.org/10.1021/bi00037a049

[42]Bassov, T., Sheves, M., Alteration of pKa of the bacteriorhodopsin protonated Schiff base. A study with model compounds, *Biochemistry*, **1980**, *25(18)*, 5249. https://doi.org/10.1021/bi00366a040

[43]Mimoum, H., Roch, I. S. D., Sajus, L., Epoxydation des olefines par les complexes peroxydiques covalents du molybdene-VI, *Tetrahedron*, **1970**, *26(1)*, 37. https://doi.org/10.1016/0040-4020(70)85005-0

[44]Conte, V., Furia, F. D., *Catalytic Oxidations with Hydrogen Peroxide as Oxidant*, Kluwer Academic Publisher, Berlin., **1992**,

[45]Mimoum, H., Saussine, L., Daire, E., Postel, M., Fisher, J., Weiss, R., Vanadium(V) peroxy complexes. New versatile biomimetic reagents for epoxidation of olefins and hydroxylation of alkanes and aromatic hydrocarbons, *J. Am. Chem. Soc*., **1983**, *105(10)*, 3101. https://doi.org/10.1021/ja00348a025

[46]Nair, M. L. H., Thankamani, D., Vanadium(V) peroxy complexes. New versatile biomimetic reagents for epoxidation of olefins and hydroxylation of alkanes and aromatic hydrocarbons, *Indian J. Chem*., **2009**, *48A*, 1212.

[47]Garner G. D., *Molybdenum*, special topics in *Comprehensive Coordination Chemistry*, Wilkinson G, Ed., Pergamon press, Oxford., **1987**, *6*, 1421.

[48]Niasari, M. S., Davar, F., Bazarganipour, M., Synthesis, characterization and catalytic oxidation of para-xylene by a manganese(III) Schiff base complex on functionalized multi-wall carbon nanotubes (MWNTs), *Dalton Trans.*, **2010,** *39(31)*, 7330. https://doi.org/10.1039/b923416k

[49]Ambroziak, K., Mbeleck, R., He, Y.,Saha, B., Sherrington, D. C., Investigation of batch alkene epoxidations catalyzed by polymer-supported Mo(VI) complexes, *Ind. Eng. Chem. Res.*, **2009**, *48(7)*, 3293. https://doi.org/10.1021/ie801171s

[50]Vogel, A. I., A *Text Book of Quantitative Inorganic Analysis*, 4th Edn., Longmans Green Co. Ltd., London., **1978**.

[51]Vogel, A. I., *A Text book of Practical Organic Chemistry*, 4th Edn., Longmans Green Co. Ltd., London., **1978**.

[52]Rana, V. B., Singh, P., Singh, D. P.,Teotia, M. P.,Trivalent chromium, manganese, iron and cobalt chelates of a tetradentate N_6 macrocyclie ligand, *Transit. Met. Chem*., **1982**, *7(3)*, 174. https://doi.org/10.1007/BF01035836

[53]Chandra, S., Sharma, K. K., Synthesis and characterization of copper(II) complexes of a macrocyclic ligand, *Transit. Met. Chem*., **1983**, *8(1)*, 1. https://doi.org/10.1007/BF00618784

[54]Malik, W. U., Bembi, R., Singh, R., Preparation and characterisation of some new 12- and 14-membered dibenzotetraaza macrocyclic complexes of iron(III), *Inorg. Chim. Acta*, **1983**, *68*, 223. https://doi.org/10.1016/S0020-1693(00)88965-3

[55]Owaik, T. G., Sobczak, L. J. J. M., Kowski, J. J. Z., New insights into the chemistry of oxomolybdenum(VI) complexes with N-salicylidene-2-aminoethanol, *Inorg. Chim. Acta*, **2003**, *356*, 387. https://doi.org/10.1016/S0020-1693(03)00301-3

[56]Ferraro, J. R., *Low Frequency Vibrations of Inorganic and Coordination Compounds*, Plenum, New York, **1971**,

[57]Dyer, J. R., *Applications of absorption spectroscopy of organic compounds*, Prentice-Hall, Inc., Englewood Cliffs, USA, **1965**,

[58]Singh S., Yadav, H. S., Yadava A. K., Rao, D. P., Synthesis and characterization of oxovanadium(IV) complexes with tetradentate Schiff base ligands having thenil as precursor molecule, *Curr. Res. Chem*., **2011**, *3(2)*, 106. https://doi.org/10.3923/crc.2011.106.113

[59]Willis, L. J., Loehr, T. M., Miller, K. F., Bruce, A. E., Stiefe, E. I., Raman and infrared spectroscopic studies of dioxomolybdenum(VI) complexes with cysteamine chelates, *Inorg. Chem*., **1986**, *25(23)*, 4289. https://doi.org/10.1021/ic00243a045

[60]Ceylan, B. I., Kurt, Y. D., Ulkuseven, B., Synthesis and characterization of new dioxomolybdenum(VI) complexes derived from benzophenone-thiosemicarbazone (H_2L). Crystal structure of [MoO_2L(PrOH)], *J. Coord. Chem*., **2009**, *62(5)*, 757. https://doi.org/10.1080/00958970802339669

[61]Rao, S. N., Kathale, N., Rao, N. N., Munshi, K. N., Catalytic air oxidation of olefins using molybdenum dioxo complexes with dissymmetric tridentate O,N,S-donor Schiff base ligands derived from o-hydroxyacetophenone and S-benzyldithiocarbazate or S-methyldithiocarbazate, *Inorg. Chim. Acta*, **2017**, *360(14)*, 4010. https://doi.org/10.1016/j.ica.2007.05.035

[62]El-Medani, S. M., Aboaly, M. M., Abdalla, H. H., Ramadan, R. M., Reactions of group 6 metal carbonyls with salicylaldehyde hydrazone, *Spectrosc. Lett*., **2004**, *37(6)*, 619. https://doi.org/10.1081/SL-200037610

[63]Zhu, X. W., Synthesis, crystal structures and catalytic property of dioxomolybdenum(VI) complexes derived from tridentate Schiff bases, *Acta Chim. Slov*., **2018,** *65(4)*, 939. https://doi.org/10.17344/acsi.2018.4607

[64]Maurya, R .C., Verma, R., Singh, T., Synthesis, magnetic, and spectral studies of some mono- and binuclear dioxomolybdenum(VI) complexes with chelating hydrazones derived from acid hydrazides and furfural or thiophene-2-aldehyde, *Synth. React. Inorg. Met-Org. Chem*., **2003**, *33*, 309. https://doi.org/10.1081/SIM-120017789

[65]Wang, X., Zhang, X. M.,Liu, H. X., Synthesis, characterization and crystal structure of cis-dioxomolybdenum(VI) complexes of the Schiff base Girard reagent (T) salt, *J. Coord. Chem*., **1994**, *33*, 223. https://doi.org/10.1080/00958979408024280

[66]Rao, D. P., Yadav, H. S., Yadava, A. K., Singh, S., Yadav, U. S., Syntheses and spectroscopic studies on macrocyclic complexes of dioxomolybdenum(VI) with di-2-furanylethanedione as precursor, *E-J. Chem*., **2012**, *9(2)*, 497. https://doi.org/10.1155/2012/205123

[67]Cotton, F. A., Wilkinson, G., Murillo, C. A., Bochmann, M., *Advanced Inorganic Chemistry*, 6thEdn., Wiley, New York, **1994**, 944.

[68]Nakamoto, K., *IR and Raman Spectra of Inorganic and Coordination Compounds, part A and B*, John Wiley and Sons, New York., **1998**,

[69]Gehrke, H., Jr., Veal, J., Acetylacetonate complexes of molybdenum(V) and molybdenum(VI), *Inorg. Chim. Acta*, **1969**, *3*, 623. https://doi.org/10.1016/S0020-1693(00)92563-5

[70]Yadav, H. S., Synthesis of spectroscopic studies of oxovanadium(IV) complexes with 16- and 18-membered macrocyclic ligands, *Polyhedron***,** **1993**, *12(3)*, 313. https://doi.org/10.1016/S0277-5387(00)81729-5

[71]Rao, D. P., Yadav, H. S., Yadava, A. K., Singh, S., Yadav, U. S., In-situ preparation of macrocyclic complexes of dioxomolybdenum(VI) involving a heterocyclic precursor, J. *Coord. Chem*., **2011**, *64(2)*, 293. https://doi.org/10.1080/00958972.2010.544037

[72]Sakata, K., Kuroda, M., Yanagida, S., Hashimoto, M., Preparation and spectroscopic properties of oxovanadium(IV) and dioxomolybdenum(VI) complexes with tetraaza[14] annulenes containing pyridine rings, *Inorg. Chim. Acta*, **1989,** *156(1)*, 107. https://doi.org/10.1016/S0020-1693(00)90375-X

[73]Garg, R., Saini, M. K., Fahmi, N., Singh, R. V., Spectroscopic and biochemical studies of some manganese(II), oxovanadium(V) and dioxovanadium(VI) complexes S/O and N donor agents synthesized under microwave conditions, *Transit. Met. Chem*., **2006,** *31*, 362. https://doi.org/10.1007/s11243-005-0001-1

[74]Kahroic, E., Molcanov, K., Tusek-Bozic, L., Kojic-Prodic, B., New complexes of Mo(V) with Schiff bases: Crystal structure of butylammonium di-μ-oxo-μ-acetato-bis[(N-butylsalicylideniminato-N,O)oxomolybdenum(V)]benzene, acetic acid solvate, *Polyhedron*, **2006**, *25*, 2459. https://doi.org/10.1016/j.poly.2006.02.008

[75]Ballhausen, C. J., Gray, H. B., The electronic structure of the vanadyl ion, *Inorg. Chem*., **1962,** *1*, 111. https://doi.org/10.1021/ic50001a022

Received: 16.08.2019

Accepted: 09.11.2019.

CHEMICAL ANALYSIS OF PIGMENT PRODUCED BY HALOALKALOTOLERANT BACTERIA *PARACOCCUS BEIBUENSIS* SL2

Deepti D. Dhere[a]* and S. M. Dharmadhikari[b]

Keywords: *Paracoccus beibuensis;* chemical analysis; pigment.

Paracoccus beibuensis SL2 is a halo-alkalotolerant bacteria isolated from Lonar Crater, Buldhana, Maharashtra, India and was identified by conventional and advanced techniques. The 16s rRNA sequence was deposited to NCBI GenBank with accession number KY129665. In recent studies the bright orange pigment produced by *Paracoccus beibuensis* SL2 was extracted and purified. The analysis of purified pigment was done by spectrophotometric method, chemical method, TLC, FT-IR and HPLC to know the chemical nature of pigment. The overall studies showed that bright orange pigment produced by *Paracoccus beibuensis* SL2 is a carotenoid group pigment which is mainly a xanthophyll pigment showing similar characters with that of Astaxanthin. It has a great commercial value as a natural colorant and therapeutic molecule.

*Corresponding Authors
E-Mail: deepti.dhere@gmail.com
[a] Deogiri College of Arts, Science and Commerce, Aurangabad, (M.S.), India
[b] Government College of Arts and Science, Aurangabad, (M.S), India

INTRODUCTION

Color is an indistinguishable character which decides aesthetic value of the matter. It is the first characteristic property perceived by senses. Color has been added to food to make it more attractive and appealing. Due to increased awareness about toxicity of synthetic colors, a demand for colors from natural origin has been increased and creating pressure to 'go natural'. Natural colors can be derived from plants and plant products but they have seasonal variation, different geographical distribution and year around availability. The microbial pigments are promising alternative to other color additives extracted from vegetables or synthetic one because it poses no seasonal variation and show high production.

Microorganisms produce various pigments like carotenoids, melanin's, flavins, monascins, violacein and indigo.[1] In recent studies the chemical analysis of the pigment produced by Haloalkalotolerant bacteria *Paracoccus beibuensis* SL2 was done. The recent studies focus on chemical characterization of bright orange pigment produced by *Paracoccus beibuensis* SL2.

MATERIALS AND METHODS

The bacteria used in this study was an orange pigment producing bacterium isolated from hypersaline-hyperalkaline soil collected from Lonar Crater, District-Buldhana, Maharashtra, India on nutrient agar (Himedia) with pH 8.5 and screened out of 105 pigmented isolates. The isolate was identified as *Paracoccus beibuensis* SL2 by 16s rRNA sequencing approach at Agharkar Research Institute, Pune, Maharashtra, India and sequence was deposited to NCBI gen bank with Accession number KY 129665. The *Paracoccus beibuensis* SL2 was stored on nutrient agar slant pH 8.5 during experimental studies.

Production and extraction of the pigment

Production medium with composition: glucose 5 g L^{-1}, meat extract 15 g L^{-1} and NaCl 10 g L^{-1} with pH 9.5 was used for production of pigment at shake flask level and fermenter level. The *Paracoccus beibuensis* SL2 was inoculated (1 %) in statistically optimized media having initial pH 9.5 and incubated at 30 °C for 72 h with shaking condition (120 rpm) in white light. The extraction was done by slight modification of the procedure used by Bhat *et al.*[2] The centrifugation of culture medium was done to separate cells at 8000 rpm for 15 min. at 4 °C. Pellet obtained was washed twice with sterile distilled water by centrifugation at 8000 rpm for 10 min. The washed cell pellet was suspended in acetone and kept overnight for pigment extraction followed by centrifugation at 8000 rpm for 10 min. at 4 °C.

The acetone extract of pigment was dried using sodium sulphate and concentrated by using vacuum evaporation at room temperature in dark. The repartition was done by using two liquid phases i.e. petroleum ether and methanol which are immiscible. 2 mL of pigment concentrate was added in 5 mL petroleum ether and partitioned with equal volume of 90 % methanol followed by shaking in separating funnel. The mixture in separating funnel kept aside until two distinct layer appears i.e. epiphase and hypophase which were further analyzed for determining its chemical nature.

Chromatographic fractionation of carotenoids

Open column chromatography (OCC) was used to separate the extract into fractions containing groups of

similar polarity.[3] A plastic syringe (20 mL) was used as column packed with silica gel 60 (60-120 mesh). The stationary phase was equilibrated by suspending in the mobile phase (hexane) by gently stirring until an even suspension was formed. Glass wool was introduced at the bottom of column and column was clamped in an upright position with the tap firmly closed. The suspension was then slowly added to the column while tapping the walls of the column gently to allow air bubbles to rise to the surface. The suspension was then allowed to settle, and the tap opened leaving the mobile phase to run out slowly until the height of the supernatant liquid reaches 2 cm above the column packing. To prepare the sample, the carotenoid extract was placed in an evaporating dish in dark till it is concentrated. The carotenoid extract was introduced as a concentrated liquid from the top of the column. The chromatogram was developed in a dark room to minimize the light's decolorizing effect on the pigment. The first aliquot of mobile phase hexane was introduced, and the tap opened to adjust the flow. A flow rate of 1 mL min^{-1} was adjusted, as recommended for conventional column chromatography by Houghton and Raman.[4] The mobile phase was allowed to move down through the column under gravity. The constituents of the extract moved through the column as bands. Separation of the carotenoid pigments was followed visually, and glass test tubes used to collect 2 mL aliquots of elute which were analysed spectrophotometrically.

Analysis of pigment by TLC

The silica gel TLC plates were used instead of simple glass slides. The marked TLC plates were then activated by placing in an oven at 80 °C for 20 min to drive off water molecules that were bonded to the polar sites on the plate. The TLC procedure was performed in dark room. The TLC plates were spotted by placing the narrow end of the capillary tube into a vial containing the pigment extract. The spotted samples were then resolved using a mobile phase (methanol: benzene: ethyl acetate 5:70:25). To develop the TLC plate, the solvent was poured into a chromatography chamber. The TLC plate was then introduced in the chromatography chamber and the plate left in the chamber until solvent had advanced to the top pencil line on the slide. The slide was then removed from the developing chamber and visualized. The immediate visualization was done by drying the TLC plates in air at room temperature followed by observation. The retention front (R_f) was calculated and compared with the R_f of the standards pigment.

Pigment identification

The carotenoid pigment identification was done by spectrophotometric analysis of acetone extract and chemical identification of chloroform extract of pigment. The absorption spectrum of purified pigment extract was measured within range of 400-600 nm using acetone as reference.

Chemical identification of the polyene group of carotenoids was done according to protocol for detection of carotenoid by Ajayi.[5] For chemical identification, 1 g dry pellet of harvested cells was taken in dry tube and 10 mL of chloroform was added and shake vigorously. The resulting extract was filtered through Whatmann filter Paper No.1. and then few drops of 85 % sulfuric acid were added and observed the presence of blue colored ring.

The FT-IR analysis was done to know the presence of IR bands of characteristic functional groups present with the carotenoid molecule extracted from *Paracoccus beibuensis* SL2. The FT-IR analysis was carried out at Government Institute of Forensic science, Aurangabad. For FT-IR analysis drop of purified pigment was placed on the face of highly polished salt plate made with KBr and scanned within 400-500 nm for IR spectra at room temperature.

Purity of extracted pigment was confirmed by using HPLC (Jasco UV-2075 Plus**)** analysis. Prior to each analysis, samples were filtered through 0.45 µ Millipore disposable sterile syringe filters. The standard solutions were injected first, followed by a 10 µL aliquot of the filtered extracted carotenoid sample. The aliquots were loaded in a HPLC column C-l8, 250 mm x 4.6 mm column, 5 mm guard column and a diode array detector. The flux rate was maintained at 0.6 mL min^{-1} and the pressure at 0.30 psi. The mobile phase was a mixture of acetonitrile, methanol, and water in the proportion 47:47:16 at 30 ˚C. The degassing of solvent system was done before use by sonication for 10 min. The pigments were separated and analyzed by measuring the absorbance at 472 nm and peak identification were achieved by comparing the retention time of samples with the retention times of the standard pigment.

RESULT AND DISCUSSION

The acetone extract showed presence of bright orange pigment. The separation techniques are employed as non-chromatographic procedures because these are advantageous in large scale preparative work. These methods are precipitation methods which helps to remove major contamination of the solvents by lipids. For separation and purification of carotenoids polar and non-polar solvents are used which separate carotenoids in to polar and non-polar pigments This method is helpful for large preparative work and to facilitate the subsequent purification of pigment by separating contaminants.

According to Britton and Young,[6] the phase separation involves partitioning of an extract between two immiscible solvent phases of different polarities. The most commonly used solvents are petrol hexane and aqueous methanol (90 %). The non-polar pigments, like carotene, carotene epoxides and esters are recovered in petrol hexane epiphase. The polar pigments like xanthophylls form the lower or hypophase. The most specific separation can sometimes be achieved by modifying the solvent composition.

For separation of various components from pigment extract of *Paracoccus beibuensis* SL2, 2 mL of concentrated pigment extract was mixed with 5mL of petroleum ether and equal volume of 90 % methanol. The epiphasic petroleum ether layer shows the presence of yellow pigment which indicates presence of non-polar pigment carotene, carotene epoxides and esters. The hypophasic methanolic layer showed maximum retention of pigment which may be xanthophylls. As the xanthophyll contains hydroxyl group, it remains in the hypophase.

Vallentyne[7] elaborated that the reason for such classification is based on the structural basis of carotenes and xanthophylls, the former does not contain any hydroxyl group while the later contains two hydroxyl groups. Carotenoid pigment containing two or more hydroxyl groups occupied the hypophasic layer and those without hydroxyl group occupied the epiphase.[7-9]

Similar extraction studies were carried out by Bhat[2] and Shatila.[10] The absorption maxima of the pigment were found to be 450 nm, and 467 nm respectively which is characteristic of carotenoid pigment. Separation of crude carotenoid extract from *Paracoccus beibuensis* SL2 deduced that, extract contained both non-polar carotenes and the more polar xanthophylls. The concentration of xanthophyll pigment was highest as compared to epiphasic carotenes in low concentration. The spectra of epiphasic carotene layer did not showed characteristic absorption pattern of carotenes and hence, hypophasic xanthophyll pigment containing layer was subjected to further processing and purification.

Chromatographic fractionation of carotenoids and TLC analysis

Isolation and purification of carotenoid was carried out using an open column chromatographic technique. Several fractions with differing polarity were obtained from open column chromatography. Spectrophotometry at 480 nm was then used to group the fractions into 5. The drawback experienced in open column chromatography was the time involved for elution. According to Houghton and Raman,[4] the long retention time in open column chromatographic technique was attributed to the water present in the stationary phase. This was attributed to the slow flow rate of elution. The reported results confirmed that fractions 1, 3 and 4 were pure fractions of astaxanthin and Figure 2 shows the absorbance of fractions collected from OCC, measured at 480 nm. The collected fractions were pooled in the form of 5 fractions as represented in Table 1. This indicates that R_f value of standard carotenoid pigment astaxanthin matches with fraction 1.

The pure fractions 1 from open column chromatography was further analyzed by UV-visible spectroscopy along with chemical identification, FT-IR and high-pressure liquid chromatography. Thin layer chromatography analysis was reported as an efficient monitoring process for qualitative identification purposes.[4] However, the disadvantage observed in the present study was the degradation of pigment on the plate because of atmospheric exposure. Upon the identification of the thin layer chromatography bands, R_f value was determined (Fig. 3).

Table 1. R_f values of different fractions of pigment

No.	Fraction	R_f	Predicted pigment
1	1-A	0.75	Astaxanthin diester
2	2-B	0.12	Unidentified
3	3-C	0.33	Free astaxanthin
4	4-D	0.51	Astaxanthin monoester
5	5-E	0.21	Unidentified

Pigment identification

Bridoux[11] mentioned that, most of carotenoid pigment absorb light maximally at three wavelengths thus resulting in three peak spectra. Liakopoulou-Kyriakides *et al.*[12] mentioned that carotenoid pigment absorbs light mainly in visible region between 400-500 nm; and the obtained absorption spectra can be used for the identification of pigment. Carotenoids that contain polyene system of 10 or 11 double bonds and shows three banded absorption spectra, in which the band of maximum intensity is located at an intermediate distance from the other two bands, thus form broad bands having fine details of a shoulder.[13]

According to Britton,[3] conjugated ketocarotenoids such as canthaxanthin, astaxanthin and echinenone, the spectrum consists of broad single maximum having no defined structure. The acetone extract of pigment was analyzed by spectrophotometer within range 400-600 nm. The extracted pigment demonstrated the presence of shoulder region with maximum absorbance at 480 nm with single peak of ketocarotenoids (Fig. 1). From λ_{max} value, this ketocarotenoid can be predicted as astaxanthin. Only one report on astaxanthin producing *Paracoccus beibuensis* SL2 is available which was isolated by Zheng *et al.*[14] from marine water, China.

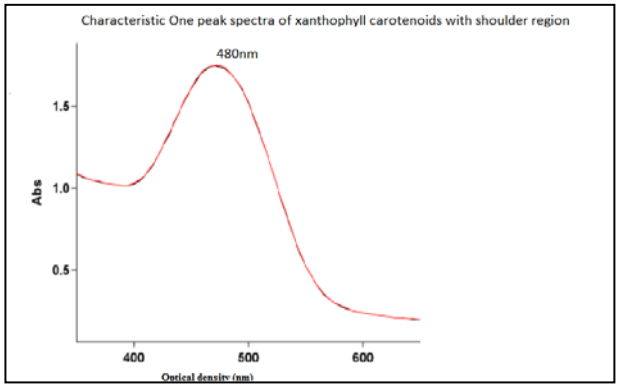

Figure 1. Spectral analysis of hypophasic pigment extract

The chemical identification of pigment extract was done by using pharmacological test for detection of carotenoid pigment as the spectrophotometric studies indicated presence of carotenoid pigments. In chemical identification, concentrated sulfuric acid gives blue-green or green-blue coloration at the interface of carotenoid extract and sulfuric acid which confirms presence of polyene group in pigment extract. The presence of polyene group confirms carotenoid nature of the pigment.

Mrak,[15] Karrer[8] and Ajayi[5] also performed the same chemical identification method for carotenoids and mentioned that the appearance of blue or violet ring at the interface between pigment extract and concentrated sulfuric acid suggest the presence of polyene pigments Similar studies on identification of chemical nature of carotenoids was done by Shatila *et al.*[10] where, the chloroform extract from *Exiguobacterium aurantiacum* FH, exhibited dark blue coloration upon the addition of concentrated sulfuric acid which revealed the presence of polyene group.

In order to understand functional groups present in pigment, FT-IR analysis of pigment was performed. The purified fraction of pigment was subjected to FT-IR analysis. The Figure 6 shows IR spectrum with major peaks at 3380, 3506, 1739, 1647, 1516 and 1349 cm^{-1} . The majority of peaks obtained on analysis showed close resemblance to ketocarotenoids. Peaks at 1739 cm^{-1} is due to >C=O and peaks at 3380 and 3506 cm^{-1} are for -OH group. The absorption in the region of 3200-2200 cm^{-1} are normally characteristic of carbon and hydrogen containing species and can be assigned to various forms of C-H stretching. The absorption above 3000 cm^{-1} suggest that the compound is likely to have unsaturated -C=C-. The absorption showing broad peak at 3380 cm^{-1} i.e. region of 3380-3506 cm^{-1} mainly occurs for -OH group. The additional intense bonds in 1647 and 1349 cm^{-1} confirms that compound consist of C=C and C-C.

The structural confirmation by IR analysis in concurrence with UV-visible analysis and reported on chemical test infer that the produced pigment is exclusively close to ketocarotenoid all aspects. Similar studies were carried out by Korumilli *et al.*[16] for structure of β-carotene extracted from *Bacillus clausii*.

Analysis of ketocarotenoid pigment by HPLC

HPLC analysis of extracted and purified pigment from strain SL2 showed presence of five peaks first four peaks were identical to peaks showed by standard carotenoid-astaxanthin. The first peak at retention time 3 min. was for all trans-astaxanthin and is major constituent of the pigment extract (Fig.7). The rest of peaks are showed asymmetrical spectra and predicted as 9-cis-astaxanthin and 13-cis-astaxanthin. According to Britton,[2] in addition to the all-trans form, carotenoids tend to isomerize and form a mixture of mono-and poly-cis isomers in homogenous solutions, where, stereochemical and energetic state decides the isomer pattern. Any compound is more resistant to isomerization when it is incorporated into the food. In general, the all-trans form of carotenoids are more rigid and most stable thermodynamically which occur predominantly in nature**.** The pigment produced by *Paracoccus beibuensis* SL2 strain was predicted as carotenoid -astaxanthin. The resulted spectra were also compared with the similar studies carried out for astaxanthin identification by Dalal *et al.*,[17] where, astaxanthin extracted from *Spingomonas astaxanthinifaciens* was identified by HPLC and showed retention time 3 min. for all trans-astaxanthin.

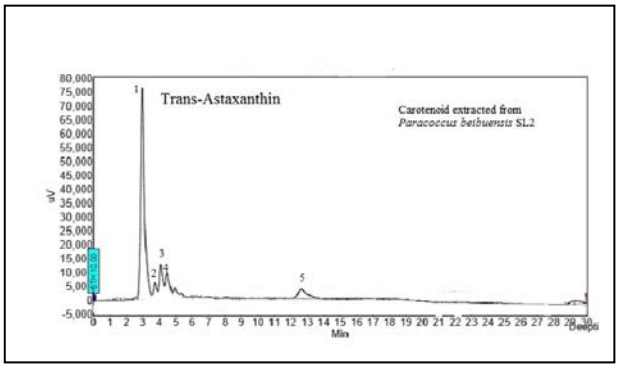

Figure 2. HPLC analysis of the purified pigment

The fractions showing λ_{max} at 480 nm were identified as carotenoid-astaxanthin, by comparing these samples to the retention times of the standard carotenoid-astaxanthin. *Paracoccus beibuensis* SL2 produces the carotenoid pigment i.e. astaxanthin as major carotenoid. Production of astaxanthin by this isolate was found to be substantive enough to prompt its biotechnological applications in the food, feed, pharmaceutical and nutraceuticals as a natural colorant.

CONCLUSION

In these studies, after extraction, separation and purification of carotenoid extract was done by using polar-non-polar solvent systems followed by open column chromatography and TLC. Majority of pigment was accumulated in lower polar alcoholic phase suggest the presence of xanthophyll group pigments. The analysis of purified extract by spectrophotometry between 400-500 nm showed one peak spectra with broad shoulder region with absorption maxima at 480 nm in acetone which is similar to carotenoid pigment-astaxanthin. FT-IR analysis of the hypophasic layer showed presence of conjugated double bonds (-C=C-), keto group (>O=C) and hydroxyl group (-OH) which again confirms xanthophyll nature of the pigment. HPLC analysis showed major peak at 3 min. which matches with peak of standard astaxanthin. From all theses it is concluded that *Paracoccus beibuensis* SL2 produces carotenoid pigment called astaxanthin.

Acknowledgement

Authors are thankful to Director, Government Institute of Science, Aurangabad, and Principal, Deogiri College, Aurangabad, Maharashtra, India for their valuable support.

This paper was presented at the "*International Symposium on Exploring New Horizons in Chemical Sciences*", January 10–12, **2019**, Aurangabad, India (ENHCS–2019).

REFERENCES

[1]Dufosse, L., *Pigments, Microbial. Encyclopedia Microbiol.* **2009**, vol. *4*, 457-471. https://doi.org/10.1016/B978-012373944-5.00155-3

[2]Bhat, M. R., Thankamani M., Media optimization, Extraction and Partial Characterization of an Orange Pigment from *Salinococcus* sp. MKJ997975. *Int. J. Life Sci. Pharm. Res.*, **2015**, *4(2)*, 85-89.

[3]Britton, G., Structure and properties of carotenoids in relation to function, *FASB J.*, 1995, 9, 1551-1558. https://doi.org/10.1096/fasebj.9.15.8529834

[4]Houghton, P. J., Raman, A., *Laboratory handbook for fractionation of natural extract*, 1st edition. Chapman and Hall, London, **1998**.

[5]Ajayi, I. A., Ajibade, O., and Oderinde, R. A., Preliminary phytochemicals analysis of some plant seeds, *Res. J. Chem. Sci*., **2011**, *1*, 58-62

[6]Britton G. and Young, A., "*Carotenoids in photosynthesis*" Springer Publications, Springer Science and Business Media, ISBN-9401121249, **2012**.

[7]Vallentyne, J. R., Epiphasic carotenoids in post-glacial lake sediments, *Limnol. Oceanogr*., **1956**, *1*, 252-262. https://doi.org/10.4319/lo.1956.1.4.0252

[8]Karrer, P. and Jucker, E., *Carotenoids.* Elsevier Publishing Company Inc., New York, Amsterdam, London, Brussels, **1950**.

[9]Fogg, G. E., and Belcher, J. H., Pigments from the bottom deposits of an English lake. *New Phytol*., **1961**, *60*, 129-142. https://doi.org/10.1111/j.1469-8137.1961.tb06246.x

[10]Fatima, S., Yusef, H., and Hanafy, H., Pigment production by *Exiguobacterium aurantiacum* FH, a novel Lebanese strain. *Int. J. Curr. Microbiol. Appl. Sci*., **2013**, *2(12)*, 176-191.

[11]Bridoux, M. C. *Algal biomarkers and their metabolites in lower food web of the great lakes, analyzed by HPLC-PDA/FL, LC-MS and GC-MS.* Ph.D. Thesis, Albany State University of New York, Proquest, USA, **2008**.

[12]Liakopoulou-Kyriakides, M. and Kyriakidis, D. A., *Croccus sativus- biological active constituents.* In: *Studies in Natural Products Chemistry: Bioactive Natural Products*.Vol.26, part C, Ur-Rahman A (Ed.), Elsevier. Amsterdam, **2002**. p. 293-312. https://doi.org/10.1016/S1572-5995(02)80009-6

[13]Fieser, L. F. Absorption spectra of carotenoids, structure, of vitamin A2. *J. Org. Chem*., **1950**, *15*, 930-943. https://doi.org/10.1021/jo01151a003

[14]Zheng, Q., Yanan, W., Chen, C., Wang, Y., Xia, X., Fu, Y., Zang, R., Jiao, N., *Paracoccus beibuensis* sp. nov., isolated from South China Sea, *Curr. Microbiol*., **2011**, *62*, 710-714. https://doi.org/10.1007/s00284-010-9768-1

[15]Mrak E. M., Phaff H. J. and Mackinney, G., A simple test for carotenoid pigments in yeasts. J. Bacteriol., **1949**, *57*, 409-411.

[16]Korumilli T. and Mishra, S., Carotenoid production by *Bacillus clausii* Using Rice Powder as sole substrate: Pigment analysis and Optimization of Key Production Parameters, *J. Biochem. Tech*., **2014**, *5(4)*, 788-794.

[17]Dalal, A., Beppu T. and Ueda, K., *Spingomonas jaspsi* sp. nov., a novel carotenoid producing bacteria isolated from Misasa, Tottori, Japan, *Int. J. Syst. Evol. Microbiol*., **2007**, 57, 1435-1441, https://doi.org/10.1099/ijs.0.64828-0

Received: 04.08.2019.
Accepted: 09.11.2019.

THERMAL BEHAVIOR OF INORGANIC HYDROGEL COMPOSITES

Sinan Temel[a], Fatma Özge Gökmen[a]* and Elif Yaman[a]

Keywords: Nano-SiO_2; TiO_2; poly(acrylic acid) (PAA); thermal behavior; hydrogels.

The objective of this work was to examine the effect of inorganic additives on thermal behavior of homo- and hetero-polymeric hydrogel. Nano SiO_2 and TiO_2 doped acrylic acid (AA) based homo-polymeric and acrylic acid/vinyl pyrrolidone (AA/VP) based hetero-polymeric hydrogels were synthesized by using in-situ free radical polymerization technique. Additives were used in the ratio of 0.005, 0.5 and 1 (wt %) on AA based homo-polymeric hydrogels. Hetero-polymeric hydrogels were prepared in ratios of 1:3, 2:2 and 3:1 (AA/VP). Additives were used in only AA/VP (3:1) and they were added 0.5 and 1 (wt %). Thermal behaviour of hydrogels, were investigated by TGA-DTA analysis. The effect of doping on pore structure of hydrogels was demonstrated by SEM analysis. SEM/EDX measurements confirmed the presence of additives in the hydrogels. The dispersions of SiO_2 and TiO_2 on hydrogel were indicated by elemental mapping and their amounts were compared with EDX analysis.

* Corresponding Authors
Fax: +90 228 214 14 27
E-Mail: fatmaozge.gokmen@bilecik.edu.tr
[a] Bilecik Şeyh Edebali University, Central Research Laboratory, Gulumbe Campus, Bilecik, Turkey.

INTRODUCTION

Polymeric materials are chosen of due to the ease of fabrication, flexibility and biocompatible nature as well as their wide range of mechanical, electrical, chemical and thermal behaviors when combined with different materials as composites.[1-3] Hydrogels are a class of wet and soft structures, composed by weakly cross-linked polymer matrixes that are hydrophilic three dimensional (3D) network.[4,5] Hydrogels provide high physical, chemical and mechanical stability in their swollen state.[6] Hydrogels have been defined which can be modified in order to achieve the unique properties. This special soft-wet structure of hydrogels makes possible them to be applied as biocompatible materials for a variety of biomedical applications including controlled drug delivery systems,[7] wound dressing,[8] coating for biosensors,[9] membranes for bio separation[10] and tissue scaffold engineering.[11] Poly(acrylic acid)(PAA) and poly(vinylpyrrolidinone)(PVP) re water soluble synthetic polymers widely used in medical applications. They have low toxicity and are used in medical, food, cosmetics and as a film forming agent.[12-14] There are many techniques reported for preparation of composites such as sol–gel, in situ dispersion polymerization processing, focused pulsed laser ablation, spin coating, blend process and in situ polymerization, etc.[15-17] Among these, in situ polymerization is a facile approach that involves less time consumption, easy preparation, low cost of production and is also easily scalable.Titanium dioxide (TiO_2) and nano-SiO_2 are considered to best choices of proficient inorganic material due to their outstanding biocompatibility and biomechanical properties (Mohanaprina).

In this study, acrylic acid (AA) and acrylic acid-*co*-vinyl pyrrolidone (VP) were used as a monomer. Nano SiO_2 and TiO_2 were added to the solution of AA and AA-*co*-VP (3:1) with the crosslinking agent and initiator, cross-linked disk-shaped nanocomposite hydrogels were obtained. The nano-SiO_2 and TiO_2 are used as inorganic reinforcement materials and they are supplied by commercially. In the preparation of nanocomposite hydrogels, AA and AA-*co*-VP monomers were preferred because of their biocompatibility properties. Both homopolymeric and heteropolymeric nanocomposite hydrogels were synthesized by using free radical in-situ polymerization method.

EXPERIMENTAL

Materials used throughout this study; nano-SiO_2 (20-30 nm), TiO_2, acrylic acid, vinyl pyrrolidone, ammonium persulfate, N,N'-methylenebisacrylamide (N,N'-MBAAm) were purchased from Sigma-Aldrich. The cross-linked homo-polymeric and hetero-polymeric hydrogels were prepared by using AA and AA-*co*-VP monomers in PVC straws. The hydrogel solution containing monomer, initiator, crosslinking agent, solvent, and also nanoparticles was heated in a temperature-controlled water bath (at 80°C) for 2 h. The experimental part was used similar to that described in our previous publication.[18]

Measurements

FT-IR analysis were recorded by Perkin Elmer, Spectrum 100 model FT-IR in the range of 400-4000 cm^{-1}. ATR mode was selected and each spectrum was scanned 4 times and worked at a resolution of 4 cm^{-1}. FESEM analyses were performed with Carl Zeiss, Supra 40VP model SEM. Prior to analysis, samples were swollen to equilibrium and then lyophilized. Lyophilized hydrogel discs were sputter coated with Au/Pd alloy. Inorganic particle distributions in nanocomposite hydrogels were determined by applying the mapping technique with the Bruker EDX detector. TGA analyses were performed with the SETARAM simultaneous TG / DTA instrument. The heating was carried out at a temperature range of 30°C-650 °C with a heating rate of 10 °C min^{-1} in N_2 atmosphere. All analyses were performed with approximately 10 mg of sample in Al_2O_3 pans.

RESULTS AND DISCUSSION

In this study, both synthetic homo-polymeric and two monomers (AA, VP) including hetero-polymeric nanocomposite hydrogels were produced using two separate reinforcing materials (SiO_2, TiO_2). Thermal behavior, chemical interaction and surface morphology of the obtained hydrogels have been examined and the results are discussed.

Thermal analysis

TGA curves of nano-SiO_2-free AA hydrogel and AA based homo-polymeric nanocomposite hydrogels with SiO_2 doped in the ratio of 0.05, 0.5 and 1 (wt %) are given in Figure 1. Mass of the 0.5 and 1 wt % SiO_2 doped nanocomposites were found to increase thermal strength. The 0.05 wt % SiO_2 addition had no effect as thermal resistance as compared to that of the pure AA hydrogel. Two-step decomposition curves were obtained at approximately 200-300 °C and 300-400 °C. In both steps 0.5 and 1 wt% SiO_2 was found to increase the heat loss mass resistance.

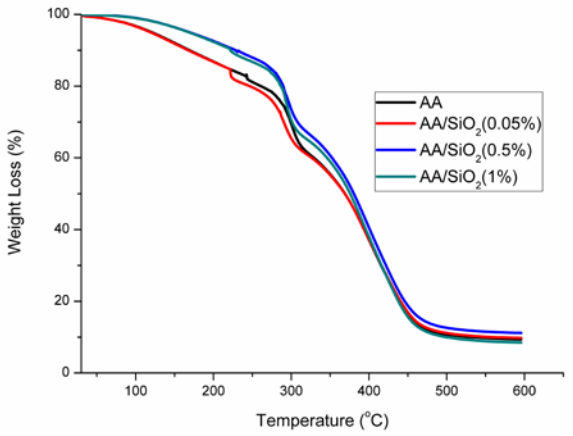

Figure 1. TGA curve of AA hydrogel and 0.05, 0.5, 1 wt % nano-SiO_2 doped AA based nanocomposite hydrogels

Figure 2 shows the TG curves of 0.05, 0.5 and 1 wt % TiO_2 doped AA hydrogels. According to this curve, the contribution of TiO_2 in the ratio of 0.05 wt % increased the thermal degradation resistance of AA based hydrogel.

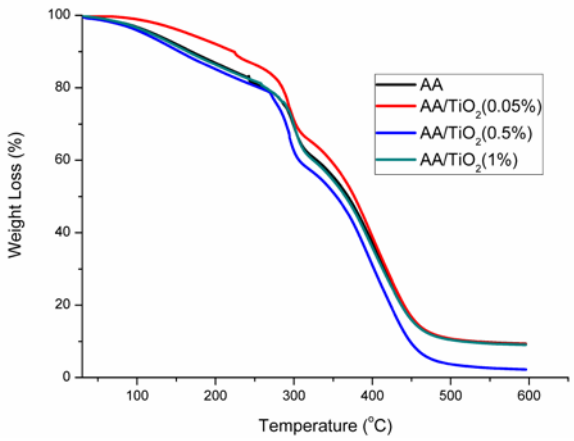

Figure 2. TGA curve of AA hydrogel and 0.05, 0.5, 1 wt% TiO_2 doped AA based composite hydrogels.

As the amount of TiO_2 increased, the thermal resistance of AA hydrogel decreased. The TiO_2 addition did not alter the 2-step chemical degradation process of the pure AA hydrogel.

Figure 3 shows the TGA curve of homo-polymeric AA hydrogel and with optimized AA/VP at a ratio of 1:3, 2:2 and 1:3. The thermal strength of the hetero-polymeric hydrogel obtained with the optimized AA/VP ratios was higher than the homo-polymeric hydrogel. With the increase of VP ratio, not only the thermal strength of the composite was increased, but also the 2-step thermal degradation behavior of acrylic acid was realized in one step. AA and AA/VP obtained in a 3:1 ratio showed similar thermal behavior. For this reason, nano-SiO_2 and TiO_2 additions were compared by applying to both hydrogels.

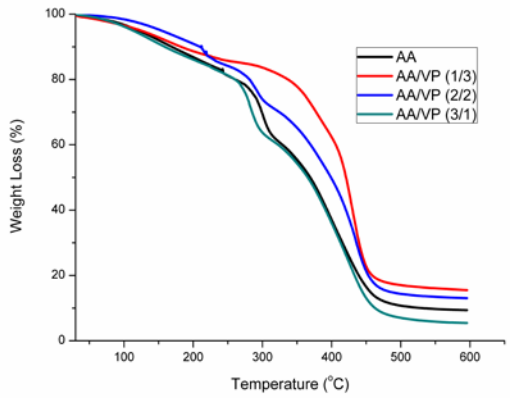

Figure 3. TGA curve of homo-polymeric AA and hetero-polymeric AA/VP in the ratio of 1:3, 2:2 and 3:1 hydrogels.

Figure 4 shows the differential thermal analysis curves of AA/VP (3:1) hetero-polymeric hydrogels with nano-SiO_2 and TiO_2 doping at 0.5 and 1% by mass. Although 0.5 wt % doped SiO_2 did not change the maximum decomposition temperature, it showed the highest thermal resistance behavior compared to other doped and undoped AA/VP (3:1) nanocomposite hydrogels. The maximum thermal decomposition temperature in the second step was most reduced in 1 wt % TiO_2 doped AA/VP (3:1) hydrogel.

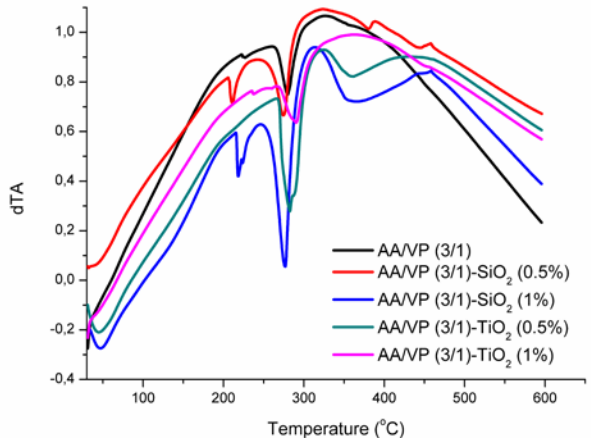

Figure 4. Differential thermal analysis of nano-SiO_2 and TiO_2 (0.5 and 1 wt %) doped and undoped hetero-polymeric AA/VP (3:1) hydrogels.

Table 1. Thermogravimetricdata of the $SiO_2$and TiO_2additive AA-homopolymericand AA/VP-heteropolymeric nanocomposite hydrogels.

AA, %	VP, %	SiO_2, wt. %	TiO_2, wt. %	degradation step, °C		$T_{d(max)}$, °C	Weight loss (%) at degradation steps, °C	
				1st	2nd		1st	2nd
100	0	-	-	30-249	249-343	245;	18	25
100	0	0.005	-	30-225	225-345	225;	16	27
100	0	0.5	-	30-275	275-342	228;	15	22
100	0	1	-	30-227	227-307	222;	11	23
100	0	-	0.05	30-240	240-297	227;	12	15
100	0	-	0.5	30-268	268-342	275	20	27
100	0	-	1	30-252	252-345	297	8	25
25	75	-	-	30-293	293-497	384;	16	67
50	50	-	-	30-222	222-308	220;	12	15
75	25	-	-	30-265	265-340	280	21	15
75	25	0.5	-	30-215	215-290	212;	13	22
75	25	1	-	30-252	252-315	215;	16	22
75	25	-	0.5	30-268	268-487	282;	18	18
75	25	-	1	30-273	273-336	292	20	21

In Table 1, the thermal decomposition steps of AA homo-polymeric hydrogel with nano-SiO_2 and TiO_2 added in mass ratios of 0.005, 0.5, 1%; AA/VP hetero-polymeric hydrogels which were prepared in different ratios (1:3, 2:2, 3:1) as well as AA/VP (3:1) hydrogel with nano-SiO_2 and TiO_2 added at a ratio of 0.5 and 1 wt%, the maximum decomposition temperatures in these steps of all samples and the percent mass losses in the thermal decomposition intervals are given. According to this table, water separation in the hydrogel structure and thermal decomposition of the hydrogel structures occurred in the first step (30-250 °C). Chemical degradation in AA and AA/VP based hydrogels occurred in 2-steps due to thermal behavior of acrylic acid.[19] Thermal degradation in the second step occurred between about 250-350 °C. As a result of the addition to homo-polymeric hydrogels, the maximum thermal decomposition was observed in the AA-TiO_2 composite hydrogel with 0.5 and 1 wt % TiO_2. There was a low increase in the 1 % TiO_2 addition at the maximum thermal decomposition temperature in the second step. Other additions did not cause a change in the maximum decomposition temperature. AA:VP hetero-polymers were prepared using AA and VP monomers in a 1:3, 2:2 and 3:1 ratio. Accordingly, as the VP amount increased, the thermal behavior changed and the maximum decomposition temperature increased by approximately 100 °C (at 384 °C).

FTIR analysis

In Figure 5, the FTIR spectrum of 1 wt % nano-SiO_2 and TiO_2 doped and undoped AA hydrogels are given. Since the chemical effect of the additives on the hydrogel were not observed in the amounts of 0.05 and 0.5 wt %, the comparison was made in 1 wt % SiO_2 and TiO_2 doping results. OH groups of the nanocomposite hydrogels gave a broad peak at approximately 2700-3600 cm^{-1}. The band at 1695 cm^{-1} is the C = O tensile vibration of the COOH group of AA. The symmetrical stress peak of Si-O-Si was observed in 1050 cm^{-1} and 441 cm^{-1} on 1 wt % SiO_2 added AA hydrogel.

The chemical interaction of Ti-O with hydrogel was not found in the spectrum because of large particle size agglomeration.

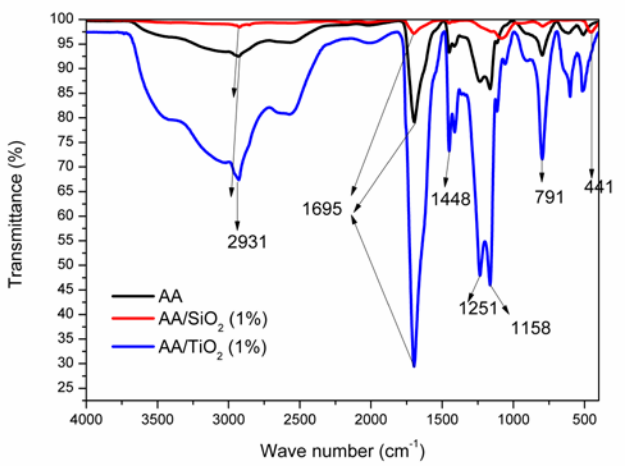

Figure 5. FTIR spectrum of 1 (wt %) nano-SiO_2 and TiO_2 doped and undoped AA hydrogel.

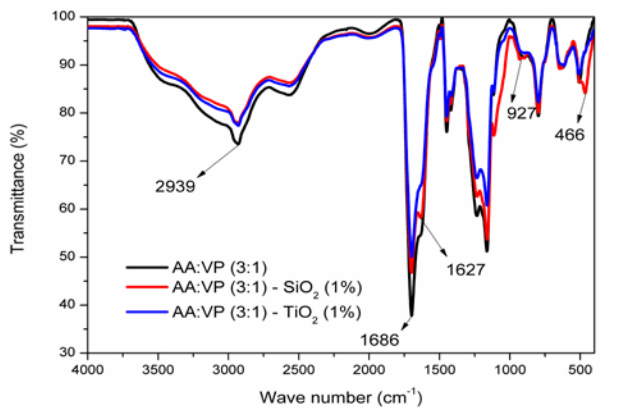

Figure 6. FTIR spectrum of 1 (wt %) nano-SiO_2 and TiO_2 doped and undoped AA/VP (3:1) hydrogels.

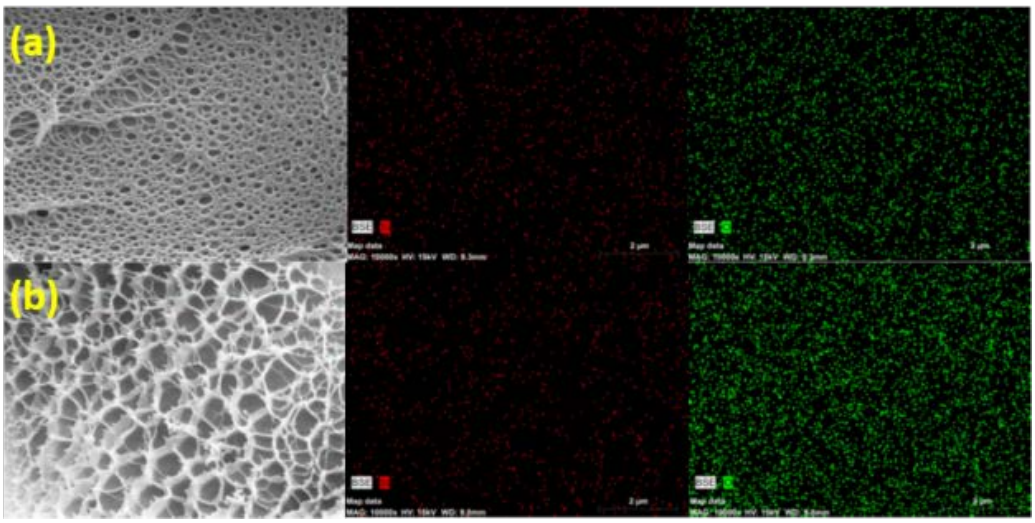

Figure 7. SEM images and elemental map distribution of (a) SiO_2 (wt %) doped AA hydrogel (b) SiO_2 (wt%) doped AA/VP (3:1) hydrogel.

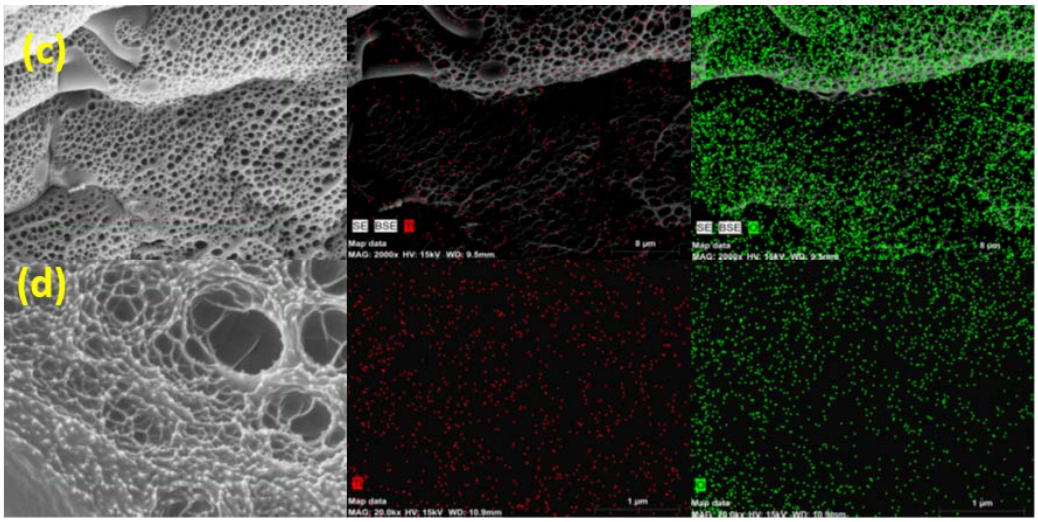

Figure 8. SEM images and elemental map distribution of (c) TiO2 (wt %) doped AA hydrogel (d) TiO2 (wt %) doped AA/VP (3:1) hydrogel.

The FTIR spectra of a 1 wt % nano-SiO_2 and TiO_2 doped and an undoped AA/VP (3:1) hetero-polymeric hydrogel's are given in Figure 6. According to spectrum, Si-O-Si stress interaction of SiO_2 doped at 466 cm^{-1} was observed. No structural change was observed in TiO_2 doped AA/VP (3:1) composite hydrogel.

SEM analysis

SEM images of SiO_2 doped AA (Fig. 7 (a)) and AA/VP (3:1) (Fig. 7 (b)) hydrogels, also silica (Si) and oxygen (O) distribution are given in Fig 7. Homogeneous pore structures were observed in both hydrogels. Si and O distributions are homogeneous on the hydrogels surface. SEM images of TiO_2 doped AA (Fig. 8 (c)) and AA/VP (3:1) (Fig. 8 (d)) hydrogel, and titanium (Ti), oxygen (O) distribution are shown in Fig 8. The pore distributions of TiO_2 doped hydrogels are not homogeneous. In the structure, the Ti and O distributions were distributed homogeneously on the polymer matrix. The EDX analysis results of all obtained samples are given in Table 2 in percent by atom. EDX signals are seen low, especially in nano-SiO_2 additive, since there is low percentage mass addition. The presence of SiO_2 on the hydrogel can be demonstrated by an increase in the total oxygen content.

CONCLUSION

It was observed that low amount (0.05 wt. %) of SiO_2 had no thermal contribution to homo-polymeric AA hydrogel. 0.5 and 1 wt% nano-SiO_2 increased the thermal degradation resistance of AA hydrogel. The TiO_2 additive, which was not used in the nanoscale, decreased the thermal strength of the AA-TiO_2 composite hydrogel, as expected, due to agglomeration as the amount of doping increased.

Table 2. Atomic % of C, O, N, Si and Ti contents in homo- and hetero-polymeric nanocomposite hydrogels.

Samples	C	O	N	Si	Ti
AA	59.11	40.89	-	-	-
AA-SiO_2 (0.05%)	57.43	42.57	-	0.00	-
AA-SiO_2 (0.5%)	57.90	42.09	-	0.00	-
AA-SiO_2 (1%)	57.63	42.34	-	0.03	-
AA-TiO_2 (0.05%)	56.74	43.23	-	-	0.03
AA-TiO_2 (0.5%)	57.52	42.47	-	-	0.01
AA-TiO_2 (1%)	60.72	39.21	-	-	0.07
AA:VP (1:3)	63.84	27.74	8.42	-	-
AA:VP (2:2)	60.55	33.63	5.82	-	-
AA:VP (3:1)	58.12	38.88	3.00	-	-
AA/VP (3:1)- SiO_2 (0.5%)	59.18	37.65	3.17	0.00	-
AA/VP (3:1)- SiO_2 (1%)	57.96	38.23	3.81	0.00	-
AA/VP (3:1)- TiO_2 (0.5%)	62.58	33.36	2.96	-	1.41
AA/VP (3:1)- TiO_2 (1%)	71.26	27.59	1.12	-	0.02

The best thermal degradation resistance was seen in AA hydrogel with 0.05 TiO_2 doped. The AA/VP hetero-polymeric hydrogel was optimized by preparing in 1:3, 2:2 and 3:1 AA:VP ratios and 3:1 AA/VP hydrogel was selected as the hydrogel. When the amount of VP increased from two different monomers, apart from the increase in thermal strength, degradation began to occur in one step. Due to the effect of reinforcing materials on hydrogels, AA and AA/VP (3:1) hydrogels with similar thermal behaviors were used as matrix in the composite.

Changing of the chemical structure of TiO_2 and SiO_2 doped homo-polymeric and hetero-polymeric hydrogels was investigated by FTIR analysis. Binding vibrations of SiO_2, homogeneously distributed on AA in nanoscale, were obtained in the FTIR spectrum. Due to the larger particle size, no structural change was observed in the same amount of TiO_2 doped AA/VP (3:1) composite hydrogel. In homo-polymeric and hetero-polymeric hydrogels, the pore and Si, O element distribution is homogeneous as a result of nano-SiO_2 doping. As a result of TiO_2 doping with large particle size, both polymer matrices lost homogeneity in pore distribution.

ACKNOWLEDGMENT

The authors thank to the Bilecik Seyh Edebali University Central Research Laboratory for the characterization measurements. Also, would like to thank Hacettepe University, Hünitek Center for TG-DTA analysis.

REFERENCES

[1] Mohanapriya, S., Mumjitha, M., Purna-Sai, K., Raj, V., Fabrication and Characterization of Poly(vinyl alcohol)-TiO_2 Nanocomposite films for Orthopaedic applications *J. Mech. Behav. Biomed.*, **2016**, *63*, 141-156. http://dx.doi.org/10.1016/j.jmbbm.2016.06.009

[2] Tanan, W., Panichpakdee, J., Saengsuwan, S., Novel Biodegradable Hydrogel Based on Natural Polymers: Synthesis, Characterization, Swelling/Reswelling and Biodegradability, *Eur. Polym. J.*, **2019**, *112*, 678-687. https://doi.org/10.1016/j.eurpolymj.2018.10.033

[3] Balasubramanian, R., Kim, S. S., Lee, J., Lee, J., Effect of TiO2 on highly elastic, stretchable UV protective nanocomposite films formed by using a combination of k-Carrageenan, xanthan gum and gellan gum, *Int. J. Biol. Macromol.*, **2019**, *123*, 1020-1027.

https://doi.org/10.1016/j.ijbiomac.2018.11.151

[4] Abdollahi, R., Taghizadeh, M. T., Savani, S., Thermal and mechanical properties of graphene oxide nanocomposite hydrogel based on poly (acrylic acid) grafted onto amylose, *Polym. Degrad. Stabil.*, **2018**, *147*, 151-158. https://doi.org/10.1016/j.polymdegradstab.2017.11.022

[5] Rasool, A., Ata, S., Islam, A., Stimuli responsive biopolymer (chitosan) based blend hydrogels for wound healing application, *Carbohyd. Polym .*, **2019**, *203*, 423-429. https://doi.org/10.1016/j.carbpol.2018.09.083

[6] Raphael, M., *Springer Science Business Media*, LLC., Springer-Verlag, New York, Kinam Park Teruo Okano, **2010**. https://www.springer.com/gp/book/9781441959188

[7] Sagiri, S. S., Singh, V. K., Kulanthaivel, S., Banerjee, I., Basak, P., Battachrya, M. K., Pal, K., Stearate organogel–gelatin hydrogel based bigels: Physicochemical, thermal, mechanical characterizations and in vitro drug delivery applications, *J. Mech. Behav. Biomed. l Mater.*, **2015**, *43*, 1–17. https://doi.org/10.1016/j.jmbbm.2014.11.026

[8] Li, D., Ye, Y., Li D., Li, X., Biological properties of dialdehyde carboxymethyl cellulose crosslinked gelatin–PEG composite hydrogel fibers for wound dressings, *Carbohydr. Polym.*, **2016**, *137*, 508–514.

https://doi.org/10.1016/j.carbpol.2015.11.024

[9] Wang, Y., Papadimitrakopoulos, F., Burgess, D. J., Polymeric "smart" coatings to prevent foreign body response to implantable biosensors, *J. Control. Release*, **2013,** *169(3)*, 341–347. https://doi.org/10.1016/j.jconrel.2012.12.028

[10] Huang, R., Kostanski, L. K., Filipe, C. D. M., Ghosh, R., Environment-responsive hydrogel-based ultrafiltration membranes for protein bioseparation, *J. Membr. Sci.*, **2009**, *336(1–2)*, 42–49.

https://doi.org/10.1016/j.memsci.2009.03.002

[11] Fan, C., Wang, D. A., A biodegradable PEG-based micro-cavitary hydrogel as scaffold for cartilage tissue engineering, *Eur. Polym. J.*, **2015,** *72*, 651–660. https://doi.org/10.1016/j.eurpolymj.2015.02.038

[12] Krezovic, B. D., Miljkovic, M. G., Stojanovic, S. T., Najman, S. J., Filipovic, J. M., Tomic, S. Lj., Structural, thermal, mechanical, swelling, drug release, antibacterial and cytotoxic properties of P(HEA/IA)/PVP semi-IPN hydrogels, *Chem. Eng. Res. Des.*, **2017**, *121*, 368-380. http://dx.doi.org/10.1016/j.cherd.2017.03.030

[13] Wang, Y., Cao, Z., Wu, J., Ma, C., Qiu, C., Zhao, Y., Shao, F., Wang, H., Zheng, J., Huang, G., Mechanically robust, ultrastretchable and thermal conducting composite hydrogel and its biomedical applications, *Chem. Eng. J.*, **2019**, *360*, 231-242. https://doi.org/10.1016/j.cej.2018.11.223

[14] Chen, K., Liu, J., Yang, X., Zhang, D., Preparation, optimization and property of PVA-HA/PAA composite hydrogel, *Mat. Sci. Eng. C-Mater. Biol. Appl.*, **2017**, *78*, 520-529. http://dx.doi.org/10.1016/j.msec.2017.04.117

[15] Hussain, F., Hojjati, M., Okamoto, M., Gorga, R. E., Review article: Polymer-matrix Nanocomposites, Processing, Manufacturing, and Application: An Overview, *J. Compos. Mater.*, **2006,** *40*, 1511–1575. https://doi.org/10.1177/0021998306067321

[17] Niu, H., Li, X., Li, H., Fan, Z., Ma, J., Guan, J., Thermosensitive, fast gelling, photoluminescent, highly flexible, and

degradable hydrogels for stem cell delivery, *Acta Biomater*., **2019**, *83*, 96-108. https://doi.org/10.1016/j.actbio.2018.10.038

[18]Mittal, H., Ray, S. S., A study on the adsorption of methylene blue onto gum ghatti/TiO2 nanoparticles-based hydrogel nanocomposite, *Int. J. Biol. Macromol*., **2016**, *88*, 66-80. http://dx.doi.org/10.1016/j.ijbiomac.2016.03.032

[19]Gökmen, F. Ö., Pekel, B. N., Synthesis and Characterization of N-[3-(Dimethylamino)propyl]methacrylamide/(nano SiO_2, amine-modified nano SiO_2, and expanded perlite) Nanocomposite Hydrogels, *Eur. Chem. Bull.,* **2017**, *6(11),* 514-418. DOI: 10.17628/ecb.2017.6. 514-518.

[20]Kabra, S., Katara, S., Rani, A., Characterization and study of Turkish perlite, *Int. J. Innov. Res. Sci. Eng. Tech.*, **2013**, *2*, 4319-4326.

Received: 24.10.2019.
Accepted: 16.11.2019

SYNTHESIS OF 1*H*-INDAZOLES USING LEMON PEEL POWDER AS A NATURAL, GREEN AND EFFICIENT CATALYST UNDER ULTRASOUND IRRADIATION

Swati S. Ghodke[a], Priya M. Khandare[a], Sadhana N. Salve[a], Pravin S. Kendrekar[b], Dhanaji Rajani[c] and Rajendra P. Pawar[a]*

Keywords: 2-substituted aldehydes, 1*H*-indazoles, hydrazine hydrate, natural catalyst, lemon peel powder (LPP).

Bioactive 1*H*-indazoles were synthesized from 2-substituted aromatic aldehydes and hydrazine hydrate using DMSO and lemon peel powder as a green and efficient natural catalyst. In comparison to other reported conventional methods, this method affords good yield under ultrasonic irradiation.

* Corresponding Authors
E-mail: kkpravin@gmail.com/rppawar@yahoo.com
[a] Department of Chemistry, Deogiri College, Station Road, Aurangabad, Maharashtra- 431005, India.
[b] Department of Health Sciences, Central University of Technology, Bloemfontein, Free State-9300, South Africa.
[c] Microcare Laboratory & Tuberculosis Research Center Surat, 395003, Gujarat, India.

INTRODUCTION

Development of efficient synthesis methods of indazole derivatives (Figure 1) has been a long-term goal in medicinal chemistry.[1-4]

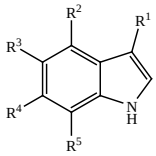

Figure 1. Structure of 1*H*-indazoles.

Among a large variety of nitrogen-containing heterocyclic compounds, indazoles are of great interest because they constitute an important class of natural and non-natural products.[5] Indazole is a nitrogen containing bicyclic heterocycle that shows a wide range of biological activities including anti-microbial,[6] anticancer,[7] antioxidant,[8] antiplatelet,[9] etc.

Owing to the biological importance, scientists have developed various methods for the synthesis of indazoles by using different catalysts such as iodine,[10] poly phosphoric acid,[11] including palladium catalyzed intramolecular amination,[12] cross coupling/cyclizations,[13] and using montmorillonite K-10.[14] Ultrasound enhances the reactivity of molecules towards many chemical reactions. Many indazoles have been synthesized by non-conventional methods[15,16] but these are more time consuming.

Lemon peel powder (LPP) is a natural and biodegradable material which can be used as a catalyst. Citric acid is present in lemon. Albedo is the major constituent of LPP.[17] The main minerals present in lemon peels includes sodium, potassium, calcium and iron.[18]

In continuation of our efforts for the eco-friendly approaches for the synthesis of bioactive heterocyclic compounds, herein we wish to report one pot synthesis of 1*H*-indazole derivatives by the reaction of an aromatic aldehyde, hydrazine hydrate and LPP as a catalyst, in DMSO, under ultrasound irradiation in a short reaction time.

EXPERIMENTAL

All the melting points were determined in open capillaries and are uncorrected. ^{1}H NMR spectra were recorded on a 500 MHz with Bruker ARS spectrometer. Chemical shifts were reported in δ ppm using tetramethyl silane as the internal standard in $CDCl_3$ solvent.

General procedure for the synthesis of substituted indazoles

A mixture of salicyldehyde (1 mmol), hydrazine hydrate (2 mmol) and LPP (10 wt %) in DMSO solvent (5 mL) was irradiated under ultra-sonication bath for appropriate time as indicated in Table 1. The progress of reaction was monitored by TLC (n-hexane: ethyl acetate, 7:3). After completion of reaction, the reaction mixture was diluted with hot ethanol and filtered. Residue, being the separated catalyst, was washed thrice (3 x 5 mL) with ethanol. The combined filtrates were concentrated to get crude product which was further purified by re-crystallization in ethanol.

Spectral data of synthesized compounds

1*H*-Indazoles was obtained by the reaction of the four 2-substituted salicyldehyde (Table 1, entry 1-4). The products exhibited almost identical spectroscopic data.

1*H*-indazole

^{1}HNMR (500 MHz, $CDCl_3$) δ = 11.10 (s,1H,NH), 8.15 (s,1H,CH), 7.36 (t,1H,Ar-H), 7.34 (dd,2H,Ar-H), 7.03 (dd,2H,Ar-H). ESI-MS: 119(M+1).

4-Chloro-1*H*-indazole (5)

^{1}H NMR (500 MHz, $CDCl_3$) δ = 11.20 (s, 1H, NH), 8.18 (s, 1H, CH), 7.53 (t,1H,Ar-H),7.25(t,1H,Ar-H),7.21(t,1H,Ar-H). ESI-MS: 153.1(M+1).

6-Chloro-1*H*-indazole (6)

^{1}HNMR (500 MHz, $CDCl_3$) δ = 12.40(s, 1H, NH), 9.01 (s, 1H, CH), 8.07 (s, 1H, Ar-H), 7.36 (d, 1H, Ar-H), 7.34 (d, 1H, Ar-H). GCMS: 153.1 (M+1).

6-Methoxy-1*H*-indazole (7)

^{1}HNMR (500 MHz, $CDCl_3$) δ = 12.41 (s, 1H, -NH), 8.14 (s, 1H, -CH), 7.95 (s, 1H, Ar-H), 7.58 (d, 1H, Ar -H), 6.87-6.90(m, 2H, Ar H), 3.40(s, 3H, CH_3). GCMS: 149.1(M+1).

4-(Diethylamino)-1*H*-indazole (8)

^{1}HNMR (500 MHz, $CDCl_3$) δ = 11.91 (s, 1H, -NH), 8.44 (s, 1H, -CH), 7.10 (d, 1H, Ar-H), 6.21-6.26 (m, 2H, Ar-H), 3.41 (q, 4H,-CH_2), 1.25 (t, 6H, -CH_3). GCMS: 190.1 (M+1).

RESULTS AND DISCUSSION

In an initial experiment, indazole was synthesized by treating a mixture of salicylaldehyde (1 mol) and hydrazine hydrate (2 mol) in DMSO (5 mL) under ultrasound irradiation in the presence of a catalytic quantity of LPP (10 % mole) for 45 min.

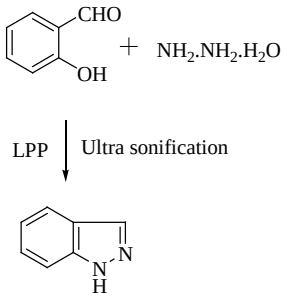

Scheme 1. General reaction for the synthesis of 1*H*-Indazole derivatives.

Table 1. Synthesis of 1*H*-indazole derivatives.

Entry	Aldehyde	Product	Time, min	Yield, %	Melting point, °C	
					Observed	Reported
1	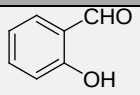	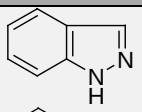	30	80	146	147[14]
2	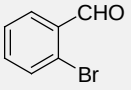	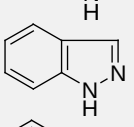	30	75	145	
3	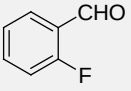	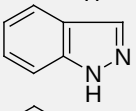	30	78	146	
4	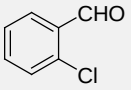	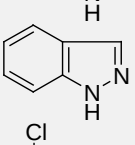	30	78	147	
5	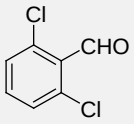	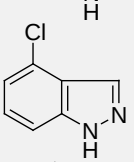	30	83	154-156	155-157[19]
6	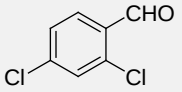	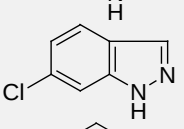	30	86	179-181	
7	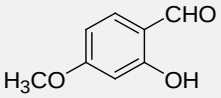	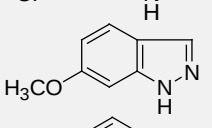	30	90	192-194	
8	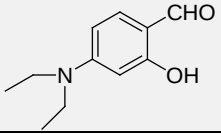	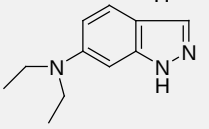	35	88	194-196	

After completion of the reaction (monitored by TLC), the LPP was filtered from the reaction mixture. The resulting filtrate was concentrated to get crude product which was recrystallized from ethanol to afford 1*H*-indazole. We optimized the effect of different solvents for the synthesis of 1*H*-indazole and observed that the best yield was obtained in DMSO (Table 2).

Table 2. Effect of various solvents on the synthesis of 1*H*-indazole.

Entry	Solvent	Yield, %
1	Water	45
2	Methanol	50
3	Ethanol	56
4	DMF	63
5	DMSO	80

Next we studied optimization of catalyst at various concentrations (Table 3). We observed that 10 wt % of catalyst was sufficient to carry out the reaction.

Table 2. Effect of catalyst on the synthesis of 1*H*-indazoles.

Entry	Catalyst, wt %	% of yield
1	2	36
2	4	50
3	6	65
4	8	76
5	10	80
6	12	80
7	14	83

Antifungal activity

Antifungal activity of the synthesized compounds was studied against fungal species *A. Niger* using carbendazim as the standard. Agar well diffusion method was used for the screening purpose. Observations were recorded after 72 h and the zone of inhibition was measured in mm at a concentration of 10 mg mL^{-1} in DMSO solvent.

Table 4. Zone of inhibition in mm of synthesized 1*H*-indazole derivatives.

Compound	Zone of inhibition, mm
1	16
2	16
3	15
4	16
5	18
6	23
7	28
8	20
STANDARD	18

CONCLUSION

In conclusion we achieved the synthesis of 1*H*-indazoles using Lemon peel powder (LPP) as an efficient natural catalyst from substituted aromatic aldehyde and hydrazine hydrate in DMSO. The conversion was very efficient and fast giving good yield of the products. All the synthesized compounds showed good to excellent antifungal activity as compare to standard carbendazim.

ACKNOWLEDGEMENT

Authors are thankful to the Principal, Deogiri College, Aurangabad, for providing necessary laboratory facilities and the Head, Department of Botany.

REFERENCES

[1]Gaikwad, D. D., Chapolikar, A. D., Devkate, C. G., Warad, K. D., Tayade, A. P., Pawar, R. P., Domb, A. J., Synthesis of indazole mofifs and their medicinal importance: An overview. *Eur. J. Med. Chem.*, **2015**, *90*, 707-731.

[2]Chandrasekhar, T., Reddy, A. B., Kumar, L. V., Naik, P. J., Sree, M. K., Swamy, G. N., Synthesis and biological evaluation of some new indazole-3-carboxamide derivatives, *Scholars Res. Library*, **2012**, *4(3)*, 1311-1316.

[3]Li, P., Wu, C., Zhao, J., Rogness, D. C., Shi, F., Synthesis of Substituted 1H-Indazoles from Arynes and Hydrazones, *J. Org. Chem.*, **2012,** *77*, 3149-3158, doi.org/10.1021/jo202598e

[4]Fang, Y., Wu, C., Larock, R. C., Shi, F., Synthesis of 2H-Indazoles by the [3+2] Dipolar Cycloaddition of Sydnones with arynes, *J. Org Chem*., **2011**, *76(21)*, 8840–8851, doi:10.1021/jo201605V

[5]Hassankhani, A., Mosaddegh, E., Ebrahimipour, S. Y., Tungstosilic acid as an efficient catalyst for the one-pot multicomponent synthesis of triazolo[1,2-a]indazole-1,3,8-trione derivatives under solvent-free condition, *Arabian J. Chem.*, **2016,** *9(1)*, 5936-5939, doi.org/10.1016/j.arabjc.2011.10.003.

[6]Parekh, C., Modi, A., Pillai, J., Patel, B., A Novel Synthesis of Series of Indazole Derivative as Potent Antimicrobial Agents, *Int. J. Drug Res. Tech.*, **2012,** *2 (3)*, 279-288.

[7]Yakaiah, T., Lingaiah, B .P. V., Narsaiah, B., Shireesha, B., Ashok, K. B., Gururaj, S., Parthasarathy, T., Sridhar, B., Synthesis and structure–activity relationships of novel pyrimido[1,2-*b*]indazoles as potential anticancer agents against A-549 cell lines, *Bioorg. Med. Chem. Lett.*, **2007**, *17(12)*, 3445-3453. doi.org/10.1016/j.bmcl.2007.03.087

[8]Polo, E., Trilleras, J., Ramos, J., Galdamez, A., Quiroga, J., Gutierrez, M., Efficient MW-assisted synthesis, spectroscopic Characterization, X-ray and antioxidant properties of indazole derivatives, *Molecules*, **2016,** *21*, 903, doi:10:3390.

[9]Bethanamudi, P., Bandari, S., Sankari, K., Velidandi, A., Chandramouli, G., Synthesis of Novel N^1 and N^2 Indazole Derivatives, *E-J. Chem.*, **2012**, *9(4)*, 1676-1682.

[10]Gaikwad, D., Abed, S., Pawar, R., Molecular iodine as an efficient catalyst for the synthesis of indazole, *Int. J. Chem. Tech. Res.*, **2009,** *1(3),* 442-445.

[11]Dennler, E., Frasca, A., Synthesis of indazoles using polyphosphoric acid-1, *Tetrahedron*, **1966,** *22(9)*, 3131-3141. doi.org/10.1016/S0040-4020(01)82291-2.

[12]Lebedev, A., Khartulyari, A., Voskoboynikov, A., Synthesis of 1-aryl-1H-indazoles via palladium-catalyzed intramolecular amination of aryl halides, *J. Org. Chem.* **2005,** *70(2)*, 596-602. doi.org/10.1021/jo048671t.

[13]Tang, X., Gao, H., Yang, J., Wu, W., Jiang, H., Efficient access to 1H-indazoles via copper-catalyzed cross-coupling/cyclisation of 2-bromoaryl oxime acetates and amines, *Org. Chem*, **2014**, *1*, 1295-1298, doi:10.1039/C4QO00244J.

[14]Hangirgekar, P., Montmorillonite K-10 catalyzed synthesis of 1-aryl-3 alkyl substituted indazoles, *J. Chem. Biol. Phys. Sci.*, **2012**, *2(4)*,1676-1680.

[15]Meng, G., Yang, T. Liu, Y., An Improved Preparation of 4-Chloro-1H indazole, *Org. Prep. Proced. Int.*, **2011,** *43*, 354-359, dx.doi.org/10.1080/00304948.2011.594005.

[16]Lukin, K., Hsu, M., Fernando, D., Leanna, M., New practical synthesis of indazoles via condensation of o-Flurobenzaldehydes and their O-methyloximes with hydrazine, *J. Org. Chem*., **2006**, *71*, 8166-8172.

[17]Pathak, P., Mandavane, S., Kulkarni, B., Fruit peel Waste: characterization and its potential uses, *Curr. Sci.*, **2017**, *113(3)*, 444-454.

[18]Janati, S., Beheshti, H., Fiezy, J., Fahim, N., Chemical composition of lemon (citrus limon) and peels its Considerations as animal and food, *GIDA: The Journal of Food*, **2012**, *37(5)*, 267-271.

Received: 13.10.2019.
Accepted: 19.11.2019.

DEVELOPMENT OF HPLC METHOD FOR DETERMINATION OF TAMSULOSIN USING QUALITY BY DESIGN (QBD) APPROACH

Jaiprakash N. Sangshetti,[a]* Dhanashree K. Chivte,[a] Mohammed Imran Anees,[a] Mallinath Langade,[b] Faraz Khan,[a] Rana Zainuddin,[a] Zahid Zaheer,[a] Paresh Mahaparale[c]

Keywords: Tamsulosin; QbD approach; RP-HPLC method; Box-Behnken model; ICH guidelines.

An HPLC method for Tamsulosin was developed by using a quality by design (QbD) novel concept. QbD has gained importance in recent times due to regulatory requirements in industrial application. Chromatographic separation of Tamsulosin was carried out by using C_8 column, and mobile phase used was methanol and distilled water (40:60 v/v) for proper separation process. Separation by using water as a solvent is beneficial as it is cost effective process and industrially applicable. In the development of the HPLC method, factors like injection volume, conc. of methanol, the column vent temperature is critical in maintaining. Hence the Box-Behnken optimization model was applied for the main, interaction and quadratic effects of these three factors on the selected response. The effect of these parameters was studied on the tailing factor (resolution). Results were analysed during a surface diagram. Verification of the software-generated result was done by taking six replicates of the run. Finally, the method was validated according to ICH guidelines.

* Corresponding Authors
E-Mail: jnsangshetti@rediffmail.com
[a] Y. B.Chavan College of Pharmacy, Dr. Rafiq Zakaria Campus, Rauza Baugh, Aurangabad-(MS) India.
[b] Jawahar Arts, Science and Commerce College, Anadur, Osmanabad (MS) India.
[c] Government College of Pharmacy, Aurangabad (MS) India.

INTRODUCTION

Tamsulosin (5-[(2R)-2-{[2-(2-ethoxyphenoxy)ethyl]-amino}propyl]-2-methoxybenzene-1-sulfonamide) acts as adrenergic α-antagonists and is maximally used to treat symptomatic benign prostatic hyperplasia (BPH), which will help with the passage of kidney stones, and also for urinary retention. Tamsulosin acts as a selective antagonist at α_{1A} and α_{1B}-adrenoceptors in the prostate, prostatic capsule, prostatic urethra, and bladder neck. The three discrete α_1-adrenoceptor subtypes such as α_{1A}, α_{1B} and α_{1D} were also identified and their distribution differs between human organs and other tissue. It was noted that there are approximately 70% of the α_1-receptors in the human prostate, which were of the α_{1A} subtype. The blockage in these types of receptors will cause relaxation of smooth muscles in the bladder neck and prostate, and which thus decreases urinary outflow resistance in males. [1]

To the best of our knowledge HPLC method using a simple UV detector by applying the QbD approach is not available. As per International Conference on Harmonization (ICH) guidance on pharmaceutical development, "QbD is a systematic approach to development that begins with predefined objectives and emphasizes product and process control and which is dependent on quality risk management and its related science.[2] QbD has gained special attention in current times due to regulatory requirements in the research work.

US-FDA has accelerated QbD drive to encourage the risk-based approach and thorough understanding of processes, which is ultimately going to help the regulatory bodies in the review process.

The basic foundation behind QbD is that quality is 'designed' into the process at the onset to the establishment of the method by a thorough understanding of the effect of the various system parameters are studied. Effects are analyzed for their influence on the quality of the product that is desired. This is nothing but ultimately to establish the design space for the method. Design space is defined as a "multidimensional combination and interaction of input variables that have been demonstrated to assure quality."[3]Some of the methods have been reported for the development of the HPLC method for Tamsulosin.[4-14]

MATERIALS AND METHODS

Tamsulosin standard active pharmaceutical ingredient (API) was procured from Hetero Drugs Limited (Hyderabad) and solvents were supplied from Dodal Enterprises and Badar chemicals, Aurangabad. Distilled HPLC grade water was prepared in the quality assurance lab of Y. B. Chavan College of Pharmacy, Aurangabad. The instrument used for HPLC analysis work was performed by using a Shimadzu LC20 model with C_8 column of 4.6×150mm; 5µmplates

Tamsulosin sample preparation

The stock solution of Tamsulosin for optimization of experiments was prepared by accurately weighing 10mg of Tamsulosin and dissolving it in 100 mL of the mobile phase composing of methanol and water 40:60 combination.

Analytical targetprofile

Quality by design approach acts as systematic approach particularly used for research in the product, process design and its development. Hence its preliminary work deals with the determination of goal or method intent. This emphasis is given on the product and process understanding.[15] Here method intent was to develop the RP-HPLC method of Tamsulosin, which is robust, accurate, precise and USP tailing factor less than 2, and analysis time, i.e., less than 10 min as per QbD norms a robust method should be developed with the help of visualized a design space.

Instrument qualification

The protocols and analytical procedures used in the pharmaceutical analysis are subjected to highly formalized validation procedures to demonstrate that they are suitable for the intended use or not. As a consequence, prior to method validation, it is essential to get assure that the equipment or analytical test system itself is adequately designed, maintained, calibrated as well as tested. These tests are called as analytical instrument qualification (AQI) which involves following qualification parameters such as

Design qualification

Installation qualification

Operational qualification

Performance qualification

In the HPLC system, it involves equipment, design qualification. Installation qualification establishes that the instrument is received as designed and that it is properly installed. As far as practical experimentation is considered, the only operational qualification and performance qualification combine parameters were done, as reported by L. K. Kaminskiet al.[16]

The precision of injection volume

It was determined by comparing the peak area received with fixed 20 µL injections and calibrated dosage loop tolerance limit set was <1 % RSD.

Injection carryover

Injection carryover was determined by running a new test directly after an analysis process and measuring possible absorption. In this, there should not be any peak from the previous analysis.

Flow rate accuracy

It was determined by measuring the volumetric flow rate of mobile phase (methanol-water 40:60 proportion) through the column over a previously set period of time such as 1.0 mL min^{-1} for 10 min, 2.0 mL min^{-1} for 5 min, 2.5 mL min^{-1} for 10 min respectively and in this the relative standard deviation (RSD) should be less than 1 %.

Flow rate precision

A flow rate precision was determined by measuring the RSD of retention times. The limit set was <1.0 % RSD.

Wavelength accuracy

It was done by scanning the compound with known specific maxima. The tolerance limit is specific maxima ±2 nm.

The linearity of the detector

The linearity of the detector was determined by injecting an increasing concentration of the substance and the tolerance limit set was $R^2 \geq 0.999$.

Risk assessment

Risk assessment deals with increase quality of method or its process management system. It also determines the various effect of its input variable on the applied method and its process. From risk assessment, one can identify with critical attributes that are going to affect the quality of the final product. A risk assessment parameter is applicable for effective communication between FDA, industries, research/development, manufacturing and multiple manufacturing sites within the company. Various tools for risk assessment are as given below:[17]

Ishikawa or fishbone diagram,

Failure model effect analysis(FMEA),

Pareto analysis.

Method design

i) Screening Method: The screening was doneby Placket-Burman Design using Design Expert 11 software.

Five factors were selected which were as follows:

1. Flow rate.
2. Injection volume.
3. Column oven temperature.
4. The concentration of methanol.
5. Detection wavelength.

The total runs obtained were 12 in number, the response for the design was tailing factor studied for the drug. The results were then put in the design to optimize the method further and chromatographic factors and response variable and Plackett-Burman design were given in Tables 1 and 2.

Table 1. Chromatographicfactors and response variable forPlackett-Burmann experimental design.

Chromatographicconditions	**Level used**	
	Low	**High**
Flow rate, mL min^{-1}	0.6	1.4
Wavelength, nm	225	235
Injection volume, µl	6	14
Concentration of methanol, %	55	65
Column oven temperature, ºC	25	35

Table 2. Plackett-Burman experimental design for Tamsulosin

Run	Factor 1	Factor 2	Factor 3	Factor 4	Factor 5	Response
	A: Flow rate, ml min^{-1}	B: Detector wavelength, nm	C: Injection volume, µL	D: Methanol concentration, %	E: Column oven temperature, ºC	Tailing factor
1	1.4	225	14	45	25	1.3
2	1.4	235	14	35	25	1.29
3	0.6	235	6	45	35	1.1
4	0.6	225	14	35	35	1.2
5	1.4	225	14	45	35	1.22
6	0.6	225	6	35	25	1.26
7	0.6	235	14	35	35	1.37
8	1.4	235	6	35	25	1.3
9	1.4	225	6	35	35	1.19
10	0.6	235	14	45	25	1.26
11	0.6	225	6	45	25	1.14
12	1.4	235	6	45	35	1.07

Optimization was done by response surface methodology and then by applying a three-level Box-Behnken design with three center points as shown in Table 3. Three factors selected were injection volume, the concentration of methanol, column oven temperature in the mobile phase. Evaluation of the mainfactor, the interaction and quadric effect on peak USP tailingfactorswere also been done. The flow rate selected for obtaining accurate results was 1ml per minute and detector wavelength was kept as 230nm as its effect on thetailingfactor was lesssignificant. Experiments were conducted by making triplicate injections (total 17 runs) of standard Tamsulosin solution as shown in Table 4. The averageof USP tailingfactor was analyzed using Design Expert 11 software.

The application of multivariate regression analysis output in a fitted full quadrate model for the average responses for peak USP tailing is accessible by the given equation

$$Y=ß_0+ ß_1X_1+ ß_2X_2+ ß_3X_3+ ß_{11}X_1^2+ ß_{22}X_2^2+ ß_{33}X_3^2+ + ß_{12}X_1X_2+ ß_{13}X_1X_3+ ß_{23}X_2X_3$$

where

Y is the response,

$ß_0$ is the arithmetic meanresponse,

$ß_1$, $ß_2$, $ß_3$ are regressioncoefficientsofthefactorX_1, X_2, X_3 respectively,

$ß_{11}$, $ß_{22}$, $ß_{33}$ are squaredcoefficients and $ß_{12}$, $ß_{13}$, $ß_{23}$ are interaction coefficients.[18]

Table 3. Chromatographic factors and response variables for Box-Behnken experimental design

Chromatographicconditions	Level used		
	Low	Centre	High
Injection volume, µL	8	10	12
Concentration of methanol, %	58	60	62
Column oven temperature, ºC	28	30	32

Critical quality attributes (CQA)

From the software-generated result, the critical factors which affect the tailing factor were determined. Factor such as flow rate, wavelength and methanol concentration in the mobile phase were found to be critical. The selection of the stationary phase was also a critical parameter. The nature of the drug is more retentive on C_8 than C_{18}.

Method validation

The chromatographic method, which was optimized and validated were according to the International Conference on Harmonization (ICH)[19] Q2 (R1) guidelines for linearity, range, precision and robustness. For the process of system suitability, a standard solution of 10µgmL^{-1} of Tamsulosin was prepared by diluting and mixing the drug with a proportion of methanol: distilled water (60:40 v/v).

A set of six replicate injection of the system standard solution was also analysed before sample analysis. The acceptance criteria for Tamsulosin were less than 2% relative standard deviation (RSD) for peak area, retention time.

Linearity

As per ICH guidelines, the linearity of an analytical procedure is defined as is its ability (within in a given range) to obtain test results that are directly proportional to the concentration (amount) of analyte in the sample. Standard calibration curves were prepared with five different concentrations by making serial volume to volume dilution of stock solution with methanol: distilled water (60:40 v/v) over the range of 10, 20, 30, 40 and 50 µg mL^{-1}.

Three replicate injections of each concentration were made to determine the linearity of Tamsulosin over the concentration range. Linear concentration curves of peak area versus drug concentration were plotted by using linear least squares regression and evaluated for linearity.

Table4. Box-Behnken methodusedfor Tamsulosin optimization

Run	Coded(X_1,X_2,X_3)	X_1: Injection volume, µL	X_2: Concentration of methanol, %	X_3:Column oven temperature, ºC
1	++0	12	62	30
2	000	10	60	30
3	-+0	8	62	30
4	0+-	10	62	28
5	--0	8	58	30
6	-0-	8	60	28
7	000	10	60	30
8	000	10	60	30
9	+0+	12	60	32
10	000	10	60	30
11	0++	10	62	32
12	+0-	12	60	28
13	0-+	10	58	32
14	000	10	60	30
15	0--	10	58	28
16	-0+	8	60	32
17	+-0	12	58	30

Table 5. Regression coefficients and associated probability values (*p*-values) for USP tailing factor of Tamsulosin (Plackett-Burman design)

Source	Sum level used				
	Sum of squares	Mean square	*F*-value	*P*-value	Significance
Model	0.077233333	0.019308333	12.91322	0.0023974	
Injection volume	0.028033333	0.028033333	18.74841	0.0034381	
Concentration of methanol	0.022533333	0.022533333	15.07006	0.0060372	Significant
Column temperature	0.013333333	0.013333333	8.917197	0.0203364	
Residual	0.010166667	0.001495238	8.917197	0.0203364	

Robustness

The robustness is defined as a measure of its capacity to remain unaffected by the small, but a deliberate change in method parameter will indicate its reliability during normal usage. There should be the reliability of the analysis with respect to deliberate variation in method parameters such as flow rate (± 0.1 mL min^{-1}), pH (±0.1 units) and mobile phase preparation.

RESULT AND DISCUSSION

Chromatographic separation was done on C-8 column (4.6×150mm, 5µm particle size) with a mobile phase of methanol and distilled water (60:40 v/v) degassed in a sonicator for 10 min and filtered through 0.2 µ membrane filter before use. Peak was obtained at 5.37 min with a flow rate of 1 mL min^{-1}, column temperature 30 ºC. Prior to the injection of drug solution, the column was equilibrated with mobile phase flowing through the system. Detection was done using a UV detector at 230nm. Further changes were made according to the optimization model and graph peak of drug is given supplementary material in.

Plackett-Burman Design

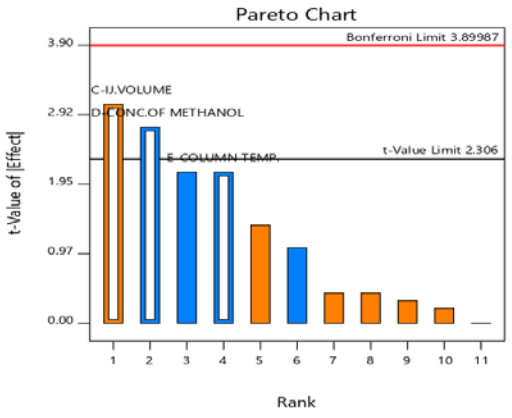

Figure 1. Pareto chart

Box-Behnken Design

Multivariate regression analysis was applied and fitted in a modified quadratic model for obtaining the USP tailing factor of the peak.

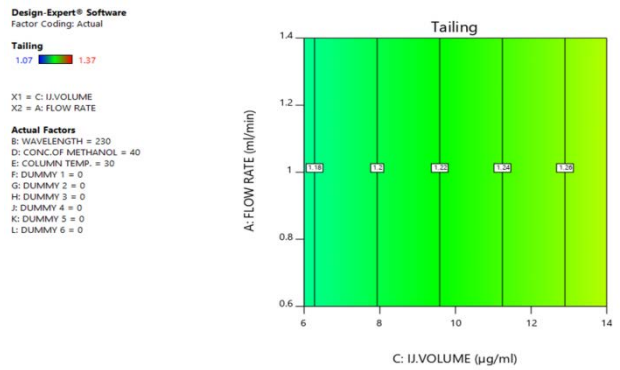

Figure 2. Tailing factor

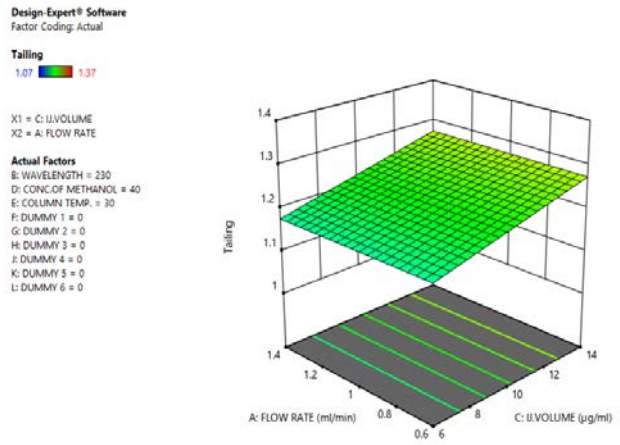

Figure 3. Response surface (3D) and contour plot showing the effect of injection volume and flow rate on USP tailing factor of Tamsulosin (Plackett-Burman Design)

Factors that were considered here were injection volumes, the concentration of methanol, column oven temperature. The regression coefficient and *P*-values derived from the software-generated report are given in Table 6. Analysis of variance (ANOVA) which was performed for study the significance of the factors and interaction terms on the response i.e. USP tailing factor of the peak, *P*-value simply provide the cut-off beyond which we assert that the findings are 'statistically significant' by convention, it is $P < 0.05$.[20]

A value of probe *F* was found to be less than 0.05, hence model was found to be significant for prediction of response. The model found was of modified quadratic model. Entire model was fitted well for optimization process and significant factors were also found which were related to Injection volume as given in Figure 1.

Response surface and contour plot were studied to visualize effect of factor and their interactions so as to develop design space for robust method and 3D graph are given in Figure 2 and 3.

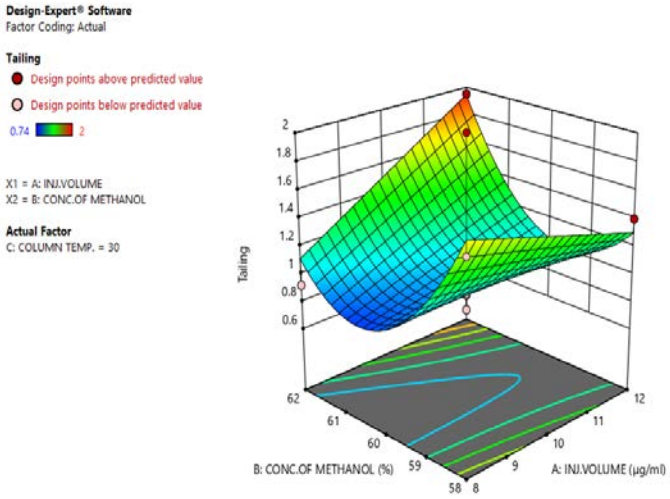

Figure 4. Response surface (3D) and contour plot showing the effects of concentration of methanol and injection volume on USP tailing factor of Tamsulosin (Box-Behnken Design)

For optimized condition, mobile phase was using in ratio of methanol: distilled water (61:39 v/v) at 230 nm wavelength having flow rate of 1 mL min^{-1} and injection volume was 10 µg mL and column temperature was set as 30 ˚C.

Method of validation

Linearity and repeatability

A set of solutions of Tamsulosin at a concentration ranging from 10 µg mL^{-1} was prepared.

Table 6. Regression coefficients and associated probability values (*P*-values) for USP tailing factor of Tamsulosin (Box-Behnken design)

Source	Sum of squares	Mean square	*F*-value	*P*-value(prob>*F*)	
Model	1.766988	0.441747	3.958307	0.028344	Significant
A-Injection volume	0.09245	0.09245	0.828405	0.030653	
B-Concentration of methanol	0.001512	0.001512	0.013553	0.909248	
AB	0.378225	0.378225	3.389113	0.90474	
BA^2	1.294801	1.294801	11.60216	0.00521	
Residual	1.3392	0.1116			
Cor total	3.106188				

Each sample was analyzed in triplicate, and the calibration curve was constructed by plotting the peak areas versus the concentration using linear regression analysis and repeatability was determined by running six replicates of samples and evaluating the average and %RSD for each sample by comparing peak area and repeatability results are given in Table 7.

Table 7. Linearity and Repeatability of Tamsulosin

Parameter	Result	Acceptance criteria
Linearity	10-50µg/ml	
Standard regressionequation	y=10043x+91076	
Repeatability	%RSD=1.18%	RSD≤2%

CONCLUSION

The quality by design approach has been successfully used to develop the HPLC method for Tamsulosin API. All critical aspects of QbD were tried to be implemented in this research study. A Systematic approach was utilized for the development of an efficient and robust method, which includes beginning with the determination of target profile characteristics, instrument qualification, risk assessment and design of the experiment. Important three factors were determined to significantly affect the peaks, which were analyzed to determine their interactions and quadratic effects with the least possible runs by using the Box-Behnken model in conjunction with response surface methodology.

Response surface diagram and contour plots were studied by which conclusions arise about which factor is affecting response with limits, which are then recorded. A desirable function was applied for the determination of optimum conditions within the parameters. Optimum conditions were obtained for the QbD approach. The one with higher desirability was selected. Replicates of the run having optimized conditions were taken to confirm the predicted response with the actual response.

ACKNOWLEDGMENTS

The authors are thankful to Honourable chairman Mrs. Fatima Rafiq Zakaria, Maulana Azad Educational Trust Dr. Rafiq Zakaria campus Chairman Aurangabad, and Principal, Y.B. Chavan College of Pharmacy, Dr. Rafiq Zakaria Campus, Aurangabad 431 001 (M.S.), India for providing all the necessary laboratory facility.

REFERENCES

[1]Q8 (R1): *Pharmaceutical Development, Revision* 1, ICH Harmonized Tripartite Guidelines, International Conference on Harmonization of Technical Requirements for Registration of Pharmaceuticals for Human Use, **2007**.

[2]Yu, L.X., Pharmaceutical Quality by design: Product and process development, Understanding and control, *Pharm. Res*., **2008**,*25*,781-791. http://dx.doi.org/10.1007/s11095-007-9511-1.

[3]Sudha, T., Dhomane, J., A validated RP-HPLC method for the determination of impurities in Tamsulosin.HCl, *Int. J. Chem. Res*., **2011**, *2(4)*,29-33.

[4]Hassan, Y., Aboul-Enein, H. Y., Hussein, R. F., Radwan, M. A., Yusuf, A., Al-Ahmadi, W., Al-Rawithi, S., Tamsulosin Dissolution from Pharmaceutical Dosage Forms Using an Automated HPLC System, *J. Liq. Chromy. Rel. Technol*., **2011**, 1109-1116, http://dx.doi.org/10.1081/JLC-120020097

[5]Bari, S. B., Bakhshi, A. R., Jain, P. S. and Surana, S. J., Development and validation of stability indicating HPTLC determination of Tamsulosin in bulk a d pharmaceutical dosage form, *Chrom. Res. Int*., **2011**, Article ID 893260 http:// dx.doi.org/10.4061/2011/893260.

[6]Israel, D. S., Krishnachaitanya, K., Sankar, D. G., RP-HPLC method for the estimation of Tamsulosin and Solifenacin in bulk and its dosage form, *Int. J. Pharm. Sci. Res.,* **2013**, *4(11),* 4343-50. http://dx.doi.org/10.13040/IJPSR.0975-8232.4(11).4343-50

[7]Kumar, G. S. and Kumar, S. P. B., Stability-indicating RP-HPLC Method for Determination of Tamsulosin.HCl in Pharmaceutical Dosage Form, *J. Basic Clin. Pharm*., **2012**, 256-260. http:// dx.doi.org/ 10.4103/0976-0105.103817

[8] Din, L., Li, L., Tao P., Zhang, Z., Quantitation of Tamsulosin in human plasma by liquid chromatography-electrospray ionization mass spectrometry, *J. Chrom., B., Anal. Technol. Biomed. Life Sci*., **2002**, *7667(1),* 75-81. http://dx.doi.org/10.1016/s0378-4347(01)00546-1.

[9]Rao, R. N., Talluri, M. V. N. K., Raju, A. N., Shinde, D. D., RAmanjaneyulu, G. S., Development of a validated RP-LC/ESI-MS-MS method for separation ,identification and determination of related substances of Tamsulosin in bulk drug and formulations, *J. Pharm. Biomed. Anal*., **2008**, *46(1),* 94-103. http://dx.doi.org/10.1016/j.jpba.2007.09.009

[10]Zhang, Z., Yang, G., Liang, G., Liu, H., Chen, Y., Chiral Seperation of Tamsulosin isomers by HPLC using cellulose tris as a chiral stationary phase, *J. Pharm. Biomed. Anal.*, **2004**, *34(3),* 689-93. http://dx.doi.org/10.1016/s0731-7085(03)0555-7.

[11]ICH Harmonized tripartite guideline pharmaceutical development Q8 (R2). d.o.i: www.ich.org.

[12]Dalal, A., Anees, M. I., Khan, F., Langade, M., Khan, F. A. K., Chabukshwar, A., Sangshetti, J. N., HPLC method development for determination of Pyrazinamide and related substances by using QbD approach, *Eur. Chem. Bull.*, **2019**, *8(10),* 328-334. http:// dx.doi.org/10.17628/ecb.2019.8.328-334.

Received: 13.10.2019.
Accepted: 11.12.2019.